ELSEVIER

Physica D 121 (1998) 317–343

PHYSICA D

Quantum weak turbulence with applications to semiconductor lasers

Y.V. Lvov [a,b,*], R. Binder [c], A.C. Newell [a,d]

[a] *Department of Mathematics, The University of Arizona, Tucson, AZ 85721, USA*
[b] *Department of Physics, The University of Arizona, Tucson, AZ 85721, USA*
[c] *Optical Sciences Center, The University of Arizona, Tucson, AZ 85721, USA*
[d] *Department of Mathematics, University of Warwick, Coventry, CV47AL, UK*

Received 15 September 1997; accepted 21 January 1998
Communicated by L. Kramer

Abstract

Based on a model Hamiltonian appropriate for the description of fermionic systems such as semiconductor lasers, we describe a natural asymptotic closure of the BBGKY hierarchy in complete analogy with that derived for classical weak turbulence. The main features of the interaction Hamiltonian are the inclusion of full Fermi statistics containing Pauli blocking and a simple, phenomenological, uniformly weak two-particle interaction potential equivalent to the static screening approximation. We find a new class of solutions to the quantum kinetic equation which are analogous to the Kolmogorov spectra of hydrodynamics and classical weak turbulence. They involve finite fluxes of particles and energy in momentum space and are particularly relevant for describing the behavior of systems containing sources and sinks. We make a prima facie case that these finite flux solutions can be important in the context of semiconductor lasers and show how they might be used to enhance laser performance.

Keywords: Quantum weak turbulence; Quantum kinetic equation; BBGKY hierarchy; Kolmogorov spectra; Semiconductor laser

1. Introduction and general discussion

1.1. Background

Gaining a good understanding of the relaxation processes of many particle (or many wave) systems is a difficult task. A successful approach requires many ingredients. First, one must make approximations concerning the relative strength and uniformity (in momentum space) of the nonlinear coupling. Second, one needs to understand how the infinite hierarchy of moment equations can effectively decouple and give rise to a closed kinetic Boltzmann equation for the redistribution of particles (waves) and energy in momentum space. One of the goals of this paper is to show that one can indeed, as one can do for classical systems, derive the quantum kinetic Boltzmann equation in a self-consistent manner without resorting to a priori statistical hypotheses or cumulant discard assumptions. Third,

* Corresponding author. Fax: +1 203 524182; e-mail: lvov@snipe.lanl.gov.

0167-2789/98/$19.00
PII: S0167-2789(98)00015-3

systems are rarely in isolation and frequently involve sources (some instability or forcing that injects particles and energy, often at specific locations in momentum space) and sinks (regions of absorption of particles and energy). Moreover, and in analogy with hydrodynamic turbulence and classical wave systems, the presence of sources and sinks dramatically changes the nature of the equilibria reached by the quantum kinetic equation. A second and major goal of this paper is to describe these equilibria and show how they can affect the output of semiconductor lasers.

Fermionic quantum systems have been studied intensively for more than five decades. Many theoretical approaches (see, e.g., [1–14]) have been developed but the common feature of all is the derivation of the quantum mechanical Boltzmann kinetic equation (henceforth referred to as the quantum kinetic equation or QKE) which describes the evolution and relaxation of the particle number, $\langle a_k^\dagger a_k \rangle$, due to collisions. It is the analog of the classical kinetic equation (KE) of wave turbulence (see, e.g., [15]) and its natural quantum extension to boson gases. The QKE accounts for phase space blocking effects (Pauli exclusion principle) and is equivalent to what one would obtain by treating the scattering cross-section using the second Born approximation. Examples of variations of this equation and its derivation include the Lenard–Balescu equation which accounts for dynamical screening effects (see, e.g., [7,8]). Other extensions include generalized scattering cross sections, such as the exchange effects (crossed diagrams), as well as T-matrix effects (see, e.g., [2,9]). T-matrix approaches are especially important in systems that allow for bound states. Further generalizations of the quantum Boltzmann equation are the various forms of the Kadanoff–Baym equations. The most general Kadanoff–Baym equations are two-time equations which describe charge-carrier correlations consistently with relaxation dynamics. The Markov approximation, which is the lowest-order gradient expansion with respect to macroscopic times, yields the familiar form of the Lenard–Balescu equation, and the additional static screening and small momentum transfer approximation yields the Landau kinetic equation. In contrast to the slow relaxation dynamics for which the Kadanoff–Baym gradient expansion is applicable, recent investigations have addressed the issue of ultrafast relaxation and the related problems of memory effects as contained in the Kadanoff–Baym equations (see, e.g., [11] and all references therein) and in the generalized Kadanoff–Baym equations of Lipavski, Spicka, and Velicky (see, e.g., [12–14]).

In all the derivations, the principal obstacle to be overcome is the closure problem. Due to the nonlinear character of the quantum mechanical Coulomb interaction Hamiltonian, the time evolution of the expectation values of two operator products such as $\langle a_k^\dagger a_k \rangle$ is determined by four operator expectation values $\langle a_{k_1}^\dagger a_{k_2}^\dagger a_{k_3} a_{k_4} \rangle$. The problem compounds. The time evolution of the N operator product expectation value is determined by $(N+2)$ operator expectation values and one is left with an infinite set of moment operator equations known as the BBGKY hierarchy. The closure problem is to find a self-consistent approximation of this infinite hierarchy which reduces the infinite set of coupled equations to an infinite set of equations which are essentially decoupled. To do this, one needs to make approximations and these almost always involve the introduction of small parameters.

In what follows we introduce one such small parameter, the relative strength $\epsilon, 0 < \epsilon \ll 1$, of the coupling coefficient T_{kk_1,k_2k_3} in the system Hamiltonian ($V = d$-dimensional system volume)

$$H = \frac{V}{(2\pi)^d} \int \mathrm{d}\mathbf{k}\, \hbar\omega_k a_k^\dagger a_k + \frac{V^3}{(2\pi)^{3d}} \frac{1}{2} \int \mathrm{d}\mathbf{k}_1\, \mathrm{d}\mathbf{k}_2\, \mathrm{d}\mathbf{k}_3\, \mathrm{d}\mathbf{k}_4\, T_{kk_1,k_2k_3} a_k^\dagger a_{k_1}^\dagger a_{k_2} a_{k_3} \delta(\mathbf{k} + \mathbf{k}_1 - \mathbf{k}_2 - \mathbf{k}_3). \tag{1.1}$$

By relative, we mean the ratio of T_{kk_1,k_2k_3} to ω_k. In other words, the linear response of the Hamiltonian is dominant over short times. This is not a trivial approximation because in order to develop a consistent asymptotic closure we need T_{kk_1,k_2k_3} to be small compared to ω_k *uniformly* in k. There are many important examples where this is not the case. For instance, for the classical nonlinear Schrödinger system (see, e.g., [16]), which describes the weak turbulence of optical waves of diffraction in a nonlinear medium, $\omega_k \propto k^2$ and $T_{kk_1,k_2k_3} = a/(4\pi^2)$, where a is a positive (negative) constant for the focusing (defocusing) case and it is clear that the ratio of T_{kk_1,k_2k_3} to ω_k

increases dramatically as $k \to 0$. This has real physical consequences. The asymptotic closure for the classical case, analogous to one we are about to derive for fermions, whose central feature is the classical kinetic equation describing resonant four-wave energy exchange, is only valid when the particles and energy are at finite k values. But the dynamics of the classical kinetic equation are such that most of the energy travels to a sink at large k and most of the particles and some energy travels to low k. Unless there is a strong damping near $\mathbf{k} = 0$, the flow of particles and energy towards $\mathbf{k} = 0$ will trigger collapsing filaments in the focusing case or build condensates in the defocusing case. In either case, unless there is strong damping near $\mathbf{k} = 0$, the weak turbulence theory of four-wave interactions breaks down. Likewise in plasmas and highly excited semiconductors, while the frequency ω_k is αk^2, the bare coupling coefficient T_{kk_1,k_2k_3} behaves as $1/k^2$ reflecting Coulomb interactions. Again, even though the carriers may be initially excited at $\mathbf{k}$ values much greater than zero, the natural dynamics of either the classical or quantum kinetic equations will lead to particle deposit at small $\mathbf{k}$. However, in both of these cases, there is another effect which modifies the T_{kk_1,k_2k_3} and brings the theory closer to the nonlinear Schrödinger case. The physical origin of this effect is screening and it is manifested as a weakened potential at long distances or small $\mathbf{k}$ values. The modification is a renormalization of the coupling coefficient T_{kk_1,k_2k_3} near $\mathbf{k} = 0$ which effectively cancels the singularity, or equivalently replaces k^{-2} by $(k^2 + \kappa^2)^{-1}$, where κ is the inverse screening length. This is the small k limit of the dynamically screened effective interaction in the Lenard–Balescu approach (see, e.g., [7]). In this paper, we do not take issue [1] with the self-consistency of this approximation because we will be introducing a sink at small k values (greater than κ) which remove the potential danger in the non-uniformity of the ratio of T_{kk_1,k_2k_3} to ω_k. This is not at all artificial. The sink is, in the semiconductor laser context, nothing other than the lasing output. In what follows, then, we assume that in the k regions of interest, the ratio of T_{kk_1,k_2k_3} to ω_k is uniformly small.

There are essentially two reasons for the successful closure of the hierarchy over long times (asymptotic closure). First, to leading order in ϵ, the cumulants (the non-Gaussian part) corresponding to the expectation values of products of N operators ($N > 2$) play no role in the long time behavior of cumulants of order $r < N$. This is a consequence of phase mixing and due to the non-degenerate nature of the dispersion relation $\omega_k = \omega(|\mathbf{k}|)$. In fact, we will find that these (zeroth order in ϵ) cumulants slowly decay. The net result is that the initial state (subject to certain smoothness conditions) plays no role in the long time dynamics. Second, and more important, the higher order (in ϵ) contributions to these N-operator cumulants, which are generated directly by the nonlinearities in the system, are dominated by products of lower order cumulants. Some of these dominant terms are supported only on certain well-defined low-dimensional (resonant) manifolds in momentum space. These are responsible for the redistribution of particle number among the different momentum states and for the slow decay in time of the leading order approximation to the cumulants of order $N > 2$. The other dominant terms are non-local and lead to a nonlinear frequency renormalization of ω_k.

As a result, we are led to a very simple and natural asymptotic closure of the BBGKY hierarchy.

1.2. *Brief discussion of principal results*

Here we list and briefly discuss the main results of this article.

1. We systematically derive evolution equations over long times ϵ^{-2}, of the order of the inverse square of the coupling strength, for the *leading order* approximations of *all* Nth order cumulants $N \geq 2$. The first of these is the QKE, a closed equation for the particle number, and is consistent with what one obtains using the Hartree–Fock

[1] The strong analogy with the nonlinear Schrödinger equation would suggest that the question of the self-consistency of the quantum weak turbulence theory without small k damping might be revisited.

approximation [2] when one takes proper account of the frequency renormalization *to order* ϵ^2. The remaining equations for the leading order behavior of the higher order cumulants decouple and can be solved by a simple renormalization of the frequency which depends only on particle number density. The first correction is the well-known Hartree–Fock self energy correction whereas the second correction is new and moreover complex. The sign of the imaginary part of the latter is positive definite as the particle number approaches an equilibrium solution of the QKE. As a result, the leading order contribution to the cumulants of order $N > 2$ (which contain information on the initial state) slowly decays. Not so the higher order corrections. We obtain specific expressions for these and show that they contain terms with cumulants of higher order, products of cumulants of order N with products of particle number and products simply containing particle number alone. Only the latter two types of terms exert a long time influence and it is this fact that leads us to a natural asymptotic closure of the hierarchy.

2. The connections with classical systems and boson systems are discussed. By analogy with results obtained in the case of the classical kinetic equation, we introduce a new four-parameter family of steady (equilibrium) solutions for the QKE. The four parameters are temperature T, chemical potential μ, particle number flow rate Q and energy density flow rate P. When $P = Q = 0$, the equilibrium solution is the well-known Fermi–Dirac distribution. For either P or Q non-zero, the distributions are the analogs of the Kolmogorov distributions of classical wave turbulence, in which particles (energy) flow from sources at intermediate momentum scales to sinks at low (high) momentum values.

   These solutions have not been considered in the fermionic context before. It turns out in fact, in contrast to the pure Kolmogorov solutions (for which $Q = 0$, $P > 0$, or $P = 0$, $Q > 0$) that the relevant equilibrium solutions of the QKE which describe (a) the finite flux of particles and a little energy between intermediate momenta at which the system is pumped and a sink at low momenta and (b) the finite flux of energy and a few particles between the intermediate momenta and the energy dissipation sink at high momenta, involve special relations between Q and P. These solutions are also new for the cases of classical wave turbulence and boson systems.
3. Again by analogy with the classical case, we introduce a simple, local approximation to the collision integral in the QKE which gives excellent qualitative results. This is known as the differential approximation (see, e.g., [16–18]) and is strictly valid only when the principal transfer of energy and particles is between close neighbors in momentum space. Its most important feature, however, is that it allows us to explore both analytically and numerically the behavior of the collision integral and thereby gain a clear qualitative picture about the nature of its steady (equilibrium) solutions.
4. We briefly examine the relevance of these results in the context of semiconductor lasers using a simplified model which assumes that any relaxation due to carrier–phonon interactions is negligible with respect to carrier–carrier interactions. We suggest that it may be advantageous to pump these lasers in a fairly narrow momentum window whose corresponding frequency is greater than the lasing frequency and allow the finite flux steady (equilibrium) solutions to carry particles and energy back to the lasing frequency via collision processes. Indeed we show that, at least for the model we use, this strategy is more efficient than pumping the system across a wide range of momenta as it is currently done. Indeed, in several numerical experiments, for equal amounts of energy pumping, we find that the laser turns on when the finite flux equilibrium is excited but fails to turn on under broad-band pumping. When the pumping is increased so that the laser turns on under the latter conditions, the output power is significantly smaller than that emitted when the finite flux solution is operative.

[2] Here, we use the term Hartree–Fock approximation in the commonly used sense, which is not identical to the strict meaning of a quantum system with a Hartree–Fock wave function. In the latter, scattering and correlations are excluded.

2. Systematic derivation of the kinetic equation and evolution equations for higher order cumulants

2.1. Basic definitions and evolution equation

We start from the Hamiltonian (1.1) of a spatially homogeneous system of particles with binary interactions. Here, $e_k = \hbar\omega_k$ is the energy level of momentum state $\mathbf{k}$ (e.g., in semiconductors, the parabolic band approximation is given by $\omega_k = \alpha\mathbf{k}^2$) where $\mathbf{k}$ is a d-dimensional wave vector, and $a_k^\dagger, a_k$ are fermionic creation/annihilation operators fulfilling the anticommutation relations,

$$a_i a_j^\dagger + a_j^\dagger a_i = \delta_{ij}, \qquad a_i a_j + a_j a_i = 0. \tag{2.1}$$

We include the size of the system in the definition of the interaction matrix element $T_{12,34}$. We introduce for convenience the short hand notation: $\mathbf{k}_1 \equiv 1$, $(V/(2\pi)^d)\,\mathrm{d}\mathbf{k}_1 \equiv \mathrm{d}1$, and $((2\pi)^d/V)\delta(\mathbf{k}_1 + \mathbf{k}_2 - \mathbf{k}_3 - \mathbf{k}_4) \equiv \delta_{34}^{12}$, $\hbar = 1$. The Hamiltonian now reads

$$H = \int \mathrm{d}1\omega_1 a_1^\dagger a_1 + \frac{1}{2}\int \mathrm{d}1234 T_{12,34} a_1^\dagger a_2^\dagger a_3 a_4 \delta_{34}^{12}.$$

If one interchanges the indices 1 and 2 or 3 and 4 in the above expression and uses the fact that the Hamiltonian is Hermitian, the following properties hold:

$$T_{12,34} = -T_{21,34} = T_{21,43} = T_{43,21}^*.$$

In the Heisenberg picture, the equations of motion are

$$\dot{a}_k = \mathrm{i}[H, a]_- \equiv i(Ha - aH) \tag{2.2}$$

which give

$$\dot{a}_k^\dagger = \mathrm{i}\omega_k a_k^\dagger + \mathrm{i}\int T_{32,10} a_3^\dagger a_2^\dagger a_1 \delta_{32}^{10}\,\mathrm{d}123 \tag{2.3}$$

and

$$\dot{a}_k = -\mathrm{i}\omega_k a_k - \mathrm{i}\int T_{01,23} a_1^\dagger a_2 a_3 \delta_{32}^{10}\,\mathrm{d}123. \tag{2.4}$$

From the Heisenberg equations of motion, one can now derive the BBGKY hierarchy of equations for the normal ordered expectation values. The first three are:

$$\frac{\mathrm{d}}{\mathrm{d}t}\rho_k = 2\,\mathrm{Im}\int T_{01,23} N_{0123}\delta_{32}^{10}\,\mathrm{d}123, \tag{2.5}$$

$$\begin{aligned}\frac{\mathrm{d}}{\mathrm{d}t}N_{1'2'3'4'} = {} & \mathrm{i}\Delta_{3'4'}^{1'2'} N_{1'2'3'4'} + \mathrm{i}\int \mathrm{d}123\big(T_{32,11'}(N_{323'4'}\delta_{2'}^{1} - N_{322'13'4'})\delta_{11'}^{32} \\ & + T_{32,12'}N_{1'3213'4'}\delta_{12'}^{32} - T_{3'1,23}N_{1'2'1234'}\delta_{13'}^{32} - T_{4'1,23}(N_{1'2'23}\delta_1^{3'} - N_{1'2'13'23})\delta_{14'}^{32}\big),\end{aligned} \tag{2.6}$$

$$\mathbf{k}_1' + \mathbf{k}_2' - \mathbf{k}_3' - \mathbf{k}_4' = 0,$$

$$\begin{aligned}\frac{\mathrm{d}}{\mathrm{d}t}N_{1'2'3'4'5'6'} &= \mathrm{i}\Delta^{1'2'3'}_{4'5'6'}N_{1'2'3'4'5'6'} + \mathrm{i}\int \mathrm{d}123[T_{32,11'}(\delta^1_{2'}N_{323'4'5'6'} - \delta^1_{3'}N_{322'4'5'6'} + N_{322'3'14'5'6'})\delta^{32}_{11'}\\ &+ T_{32,12'}(\delta^1_{3'}N_{1'324'5'6'} - N_{1'323'14'5'6'})\delta^{32}_{12'}\\ &+ T_{32,13'}N_{1'2'3214'5'6'}\delta^{32}_{13'} - T_{4'1,23}N_{1'2'3'1235'6'}\delta^{4'1}_{23}\\ &- T_{5'1,23}(\delta^1_{4'}N_{1'2'3'236'} - N_{1'2'3'14'236'})\delta^{5'1}_{23}\\ &- T_{6'1,23}(\delta^1_{5'}N_{1'2'3'4'23} - \delta^1_{4'}N_{1'2'3'5'23} + N_{1'2'3'14'5'23})\delta^{6'1}_{23}],\end{aligned} \tag{2.7}$$

$$\mathbf{k}'_1 + \mathbf{k}'_2 + \mathbf{k}'_3 - \mathbf{k}'_4 - \mathbf{k}'_5 + \mathbf{k}'_6 = 0,$$

where

$$\Delta^{12}_{34} \equiv (\omega_{k_1} + \omega_{k_2} - \omega_{k_3} - \omega_{k_4}), \qquad \Delta^{123}_{456} \equiv (\omega_{k_1} + \omega_{k_2} + \omega_{k_3} - \omega_{k_4} - \omega_{k_5} - \omega_{k_6}). \tag{2.8}$$

Here, the expectation value is taken with respect to an arbitrary initial state Φ, i.e.,

$$\begin{aligned}&\rho(k_1)\delta^1_2 = \langle\Phi|a^\dagger_1 a_2|\Phi\rangle, \qquad N_{1234} = \langle\Phi|a^\dagger_1 a^\dagger_2 a_3 a_4|\Phi\rangle,\\ &N_{123456} = \langle\Phi|a^\dagger_1 a^\dagger_2 a^\dagger_3 a_4 a_5 a_6|\Phi\rangle, \qquad N_{12345678} = \langle\Phi|a^\dagger_1 a^\dagger_2 a^\dagger_3 a^\dagger_4 a_5 a_6 a_7 a_8|\Phi\rangle.\end{aligned} \tag{2.9}$$

In the definitions of these $2m$ ($m = 1, 2, \ldots$) order expectation values, the first m indices correspond to creation operators and the last m indices correspond to annihilation operators. The number of creation and number of annihilation operators are equal to each other because the Hamiltonian (1.1) conserves number of particles. The fact that the right-hand sides of (2.9) are zero on $\mathbf{k}_1 + \mathbf{k}_2 - \mathbf{k}_3 - \mathbf{k}_4 = 0$, $\mathbf{k}_1 + \mathbf{k}_2 + \mathbf{k}_3 - \mathbf{k}_4 - \mathbf{k}_5 - \mathbf{k}_6 = 0$, respectively, is a direct consequence of the spatial homogeneity of the system. This means that the Nth order moment of the spatially dependent field operators $\psi^\dagger(\mathbf{x}_j)$, $\psi(\mathbf{x}_j)$, the generalized Fourier transforms of the creation and annihilation operators $a^\dagger(\mathbf{k}_j)$, $a(\mathbf{k}_j)$, depends only on the relative spacing; i.e., on the differences of the coordinates $\mathbf{x}_j$, $j = 1, \ldots, N$.

2.2. *Cumulants and their evolution*

Let us define the cumulant of the N product of spatially dependent field operators $\psi(\mathbf{x}_j)$, $j = 1, 2, \ldots, N$, to be the moment of order N from which the appropriate combinations of products of lower order moments are subtracted so that the resulting expression has the property that it decays to zero as the separations $\mathbf{x}_j - \mathbf{x}_i$ become large. The Fourier transforms of these cumulants are therefore well-defined and these are the objects $\rho(k), \mathcal{P}_{1234}, \ldots$ with which we deal. Moreover, if the statistics are exactly Gaussian (namely, Hartree–Fock like), then all cumulants of order N, $N > 2$, are zero. Because these weakly interacting fermionic systems relax to a near Gaussian state, the cumulants are the most convenient dependent variables.

For the two- and three-particle functions we define the fourth and sixth order cumulants $\mathcal{P}_{1234}$ and $\mathcal{Q}_{123456}$, respectively, by

$$N_{1234} = \rho_1\rho_2(\delta^2_3\delta^1_4 - \delta^2_4\delta^1_3) + \mathcal{P}_{1234}\delta^{12}_{34} \tag{2.10}$$

and

$$\begin{aligned}N_{123456} &= \rho_1\rho_2\rho_3 \cdot (\delta^3_4(\delta^2_5\delta^1_6 - \delta^1_5\delta^2_6) + \delta^3_5(\delta^2_6\delta^1_4 - \delta^2_4\delta^1_6) + \delta^3_6(\delta^1_5\delta^2_4 - \delta^1_4\delta^2_5))\\ &+ \rho_3[+\mathcal{P}_{1256}\delta^3_4\delta^{12}_{56} - \mathcal{P}_{1246}\delta^3_5\delta^{12}_{46} + \mathcal{P}_{1245}\delta^3_6\delta^{12}_{45}]\\ &+ \rho_2[-\mathcal{P}_{1356}\delta^2_4\delta^{13}_{56} + \mathcal{P}_{1346}\delta^2_5\delta^{13}_{46} - \mathcal{P}_{1345}\delta^2_6\delta^{13}_{45}]\\ &+ \rho_1[+\mathcal{P}_{2356}\delta^1_4\delta^{23}_{56} - \mathcal{P}_{2346}\delta^1_5\delta^{23}_{46} + \mathcal{P}_{2345}\delta^1_6\delta^{23}_{45} + \mathcal{Q}_{123456}\delta^{123}_{456}].\end{aligned} \tag{2.11}$$

The expressions are analogs to what one would obtain in the classical case. There, the symbols $a^\dagger$ and a are complex numbers (as opposed to operators in the quantum case) and one defines the cumulants by expanding the fourth order moments into all possible decompositions; namely

$$\langle a_1^* a_2^* a_3 a_4 \rangle = \{a_1^* a_3\}\{a_2^* a_4\}\delta_3^1\delta_4^2 + \{a_1^* a_4\}\{a_2^* a_3\}\delta_4^1\delta_3^2 + \{a_1^* a_2^* a_3 a_4\}\delta_{34}^{12}, \tag{2.12}$$

where angle brackets denote moments and curly brackets denote the corresponding cumulants. In the classical case, it is consistent, but not necessary (one can keep the other terms and discover that they play no essential role), to set all correlations such as $\{a_1^* a_2^*\}$ and $\{a_3 a_4\}$ equal to zero. In the quantum case, one also decomposes $\langle \Phi | a_1^\dagger a_2^\dagger a_3 a_4 | \Phi \rangle$ into products of *all* possible decompositions. Again, it is consistent, but not necessary, to set terms such as $\{a_1^\dagger a_2^\dagger\}$ and $\{a_3 a_4\}$ equal to zero. The resulting decomposition should be consistent with the anticommutation relations (2.1), from which follows that $N_{1234} = -N_{2134}$. Therefore, certain terms (e.g., $\rho_1\rho_2\delta_4^2\delta_3^1$) are negative in (2.10), (2.11).

A general algorithm for the decomposition of the Nth order expectation value is given in Appendix A.

Having defined the higher order cumulants, we can now write down the evolution equations for the cumulant hierarchy. For the purpose of deriving the QKE, it is sufficient to consider only the equations for ρ_k and $\mathcal{P}_{1234}$. To obtain the frequency corrections to order ϵ^2 (ϵ, $0 < \epsilon \ll 1$, is a measure of the strength of the coupling coefficient), we need to consider contributions coming from the equation for $\mathcal{Q}_{123456}$. In carrying out the analysis on ρ_k, $\mathcal{P}_{1234}$ and $\mathcal{Q}_{123456}$, one finds, just as in the classical case, that certain patterns emerge which allow one to identify the terms in the equations for the cumulants of arbitrary high order that gives rise to long time effects. Taking account of these terms gives expansions (2.16) and (2.17) which will be discussed in Section 2.3. In this section we only write down equations for ρ_k and $\mathcal{P}_{1234}$. They are

$$\frac{\mathrm{d}}{\mathrm{d}t}\rho_{k_0} = 2\,\mathrm{Im}\int T_{01,23}\mathcal{P}_{0123}\delta_{23}^{01}\,\mathrm{d}123, \tag{2.13}$$

where Im denotes the imaginary part and the symbol zero denotes $\mathbf{k}$, and

$$\begin{aligned}
\frac{\mathrm{d}}{\mathrm{d}t}\mathcal{P}_{1'2'3'4'} &= \mathrm{i}\tilde{\Delta}_{3'4'}^{1'2'}\mathcal{P}_{1'2'3'4'} - (\dot{\rho}_{1'}\rho_{2'} + \rho_{1'}\dot{\rho}_{2'})(\delta_{3'}^{2'}\delta_{4'}^{1'} - \delta_{3'}^{1'}\delta_{4'}^{2'}) \\
&\quad + \underline{2\mathrm{i}T_{4'3',2'1'}\rho_{3'}\rho_{4'}(1-\rho_{2'}-\rho_{1'}) + 2\mathrm{i}T_{4'3',2'1'}\rho_{1'}\rho_{2'}(\rho_{3'}+\rho_{4'}-1)} \\
&\quad + \mathrm{i}\int \mathrm{d}123[T_{32,11'}\mathcal{P}_{323'4'}\delta_{2'}^1\delta_{11'}^{32} - T_{4'1,23}\mathcal{P}_{1'2'23}\delta_{3'}^1\delta_{14'}^{32} \\
&\quad - T_{32,11'}\cdot(\rho_2'(+\mathcal{P}_{323'4'}\delta_1^{2'} - \mathcal{P}_{3214'}\delta_{3'}^{2'} + \mathcal{P}_{3213'}\delta_{4'}^{2'}) \\
&\quad + \rho_2(\mathcal{P}_{32'14'}\delta_{3'}^2 - \mathcal{P}_{32'13'}\delta_{4'}^2) + \rho_3(-\mathcal{P}_{22'14'}\delta_{3'}^3 + \mathcal{P}_{22'13'}\delta_{4'}^3) + \underline{\underline{\mathcal{Q}_{322'13'4'}}})\delta_{11'}^{32} \\
&\quad + T_{32,12'}\cdot(\rho_2(-\mathcal{P}_{1'314'}\delta_{3'}^2 + \mathcal{P}_{1'313'}\delta_{4'}^2) + \rho_3(+\mathcal{P}_{1'214'}\delta_{3'}^3 - \mathcal{P}_{1'213'}\delta_{4'}^3) \\
&\quad + \rho_1'(+\mathcal{P}_{323'4'}\delta_1^{1'} - \mathcal{P}_{3214'}\delta_{3'}^{1'} + \mathcal{P}_{3213'}\delta_{4'}^{1'}) + \underline{\underline{\mathcal{Q}_{1'3213'4'}}})\delta_{12'}^{32} \\
&\quad - T_{3'1,23}(\rho_1(+\mathcal{P}_{1'2'23}\delta_{4'}^1) + \rho_2'(-\mathcal{P}_{1'134'}\delta_2^{2'} + \mathcal{P}_{1'124'}\delta_3^{2'} - \mathcal{P}_{1'123}\delta_{4'}^{2'}) \\
&\quad + \rho_1'(+\mathcal{P}_{2'134'}\delta_2^{1'} - \mathcal{P}_{2'124'}\delta_3^{1'} + \mathcal{P}_{2'123}\delta_{4'}^{1'}) + \underline{\underline{\mathcal{Q}_{1'2'1234'}}})\delta_{13'}^{32} \\
&\quad + T_{4'1,23}(\rho_1(+\mathcal{P}_{1'2'23}\delta_3^1) + \rho_2'(-\mathcal{P}_{1'123}\delta_{3'}^{2'} + \mathcal{P}_{1'13'3}\delta_2^{2'} - \mathcal{P}_{1'13'2}\delta_3^{2'}) \\
&\quad + \rho_1'(+\mathcal{P}_{2'123}\delta_{3'}^{1'} - \mathcal{P}_{2'13'3}\delta_2^{1'} + \mathcal{P}_{2'13'2}\delta_3^{1'}) + \underline{\underline{\mathcal{Q}_{1'2'13'23}}})\delta_{14'}^{32}],
\end{aligned} \tag{2.14}$$

on $\mathbf{k}_{1'} + \mathbf{k}_{2'} = \mathbf{k}_{3'} + \mathbf{k}_{4'}$, and the Hartree–Fock self-energy is

$$\tilde{\Delta}^{1'2'}_{3'4'} = \omega_{1'} + \omega_{2'} - \omega_{3'} - \omega_{4'} + 2\int \mathrm{d}1((T_{1'1,11'} + T_{2'1,12'} - T_{3'1,13'} - T_{4'1,14'})n_1).$$

At this stage, it is worthwhile pointing out precisely those terms, underlined in (2.14) that give rise to the various long term effects:

1. The terms that give rise to particle number transfer in the QKE are

$$2\mathrm{i}T_{4'3',2'1'}\rho_{3'}\rho_{4'}(1 - \rho_{2'} - \rho_{1'}) + 2\mathrm{i}T_{4'3',2'1'}\rho_{1'}\rho_{2'}(\rho_{3'} + \rho_{4'} - 1).$$

The reason is that when one solves for $\mathcal{P}_{1234}$, one obtains an expression which contains this term multiplied by

$$A_t(\Delta^{1'2'}_{3'4'}) = \int_0^t \mathrm{d}\tau \exp[\mathrm{i}\Delta^{1'2'}_{3'4'}t] = (\mathrm{i}\Delta^{1'2'}_{3'4'})^{-1}(\exp(\mathrm{i}\Delta^{1'2'}_{3'4'}t) - 1).$$

In the long time limit,

$$\lim_{t\to\infty} A_t(x) = \pi \operatorname{sgn} t \cdot \delta(x) + \mathrm{i}P\left(\frac{1}{x}\right).$$

Under the operator Im in (2.13), the delta function is counted twice, and the principal value term cancels. The observant reader will notice that the QKE can be effectively derived by simply ignoring all terms in the equation for $\mathcal{P}_{1'2'3'4'}$ (except $\mathrm{i}\Delta^{1'2'}_{3'4'}\mathcal{P}_{1'2'3'4'}$) proportional to cumulants of order greater than 2. In the literature, this is called the Hartree–Fock approximation. What we show in this paper is that, for the magnitude ϵ of the coupling coefficient uniformly (in $\mathbf{k}$) small, the Hartree–Fock approximation is indeed self-consistent when one takes proper account of the frequency renormalization *to order* ϵ^2.

2. The order ϵ renormalizations to the frequency come from the decomposition of sixth order moments such as $N_{1'2'13'23}\delta^{23}_{11'}$ in (2.7). These give rise to terms in the equation for $\mathcal{P}_{1'2'3'4'}$ which are proportional to $\mathcal{P}_{1'2'3'4'}$ itself. Indeed one obtains one such contribution from each of the sixth order moments in (2.7) leading to an expression in the equation for $\mathcal{P}_{1'2'3'4'}$ equal to

$$2\mathrm{i}\int \mathrm{d}1(T_{1'1,11'} + T_{2'1,12'} - T_{3'1,13'} - T_{4'1,14'})\rho_1.$$

When added to the frequency factor $\mathrm{i}(\omega_{1'} + \omega_{2'} - \omega_3 - \omega_4)$, we obtain the term denoted by $\tilde{\Delta}^{1'2'}_{3'4'}$ in (2.14). It is not too difficult to see that, in the equation for every cumulant Q_N, there is a term proportional to

$$\mathrm{i}Q_N \sum_{i=1}^{N}\left(\omega_j + 2\int T_{j1,1j}\rho_1 \,\mathrm{d}1\right),$$

and this gives rise to the first contribution in the renormalization of the frequency (2.22). In the literature, $\tilde{\Delta}^{1'2'}_{3'4'}$ is called Hartree–Fock self-energy for fourth order averages.

3. The order ϵ^2 terms in the renormalization to the frequency arise from the terms

$$\mathrm{i}\int (T_{32,11'}Q_{322'13'4'}\delta^{32}_{11'} + T_{32,12'}Q_{1'3213'4'}\delta^{32}_{12'} \quad + T_{3',23}Q_{1'2'1234'} + T_{3'1,23}Q_{1'2'13'23}\delta^{32}_{13'})\,\mathrm{d}123 \quad (2.15)$$

containing the sixth order cumulants in (2.14). The equations for the sixth order cumulant contain, in addition to terms proportional to a product of lower order particle number densities, terms proportional to $\mathcal{P}_{1'2'3'4'}$ with a factor containing $\rho_k(1 - \rho_k)$.

4. All other terms are integrals which contain highly oscillatory factors which, because of the Riemann–Lebesgue lemma, contribute nothing in the long time limit.

2.3. Asymptotic expansions and closure

We take advantage of the small parameter, the strength ϵ of the coupling coefficient and make the formal substitution $T_{12,34} \to \epsilon T_{12,34}$. We expand all cumulants Q_N in an asymptotic expansion

$$Q_2 \equiv \rho_k = n_k + \epsilon Q_2^{(1)} + \epsilon^2 Q_2^{(2)} + \cdots \tag{2.16}$$

and

$$Q_N(k_1, k_2, k_3 \ldots k_N; t) = Q_N^{(0)} + \epsilon Q_N^{(1)} + \epsilon^2 Q_N^{(2)} + \ldots, \qquad N > 2. \tag{2.17}$$

Owing to resonant interactions, these asymptotic expansions will be non-uniform in time. Namely, terms proportional to $\epsilon t, \epsilon^2 t$, etc. will appear in Q_N. These terms are removed and the asymptotic expansions (2.16) and (2.17) rendered well-ordered by allowing corrections to the time dependence of the leading order cumulants n_k, $Q_N^{(0)}$, $N > 2$. We make the ansatz

$$\frac{\partial n_k}{\partial t} = \epsilon^2 F_2^{(2)} + \ldots, \tag{2.18}$$

$$\frac{\partial Q^{(0)}_{1,2,\ldots N}}{\partial t} = \mathrm{i}(\omega_1 + \omega_2 + \cdots - \omega_N) Q^{(0)}_{1,2,\ldots,N} + \epsilon F^{(1)}_{1,2,\ldots,N} + \epsilon^2 F^{(2)}_{1,2,\ldots,N} + \cdots, \tag{2.19}$$

and choose $F_2^{(2)}$, $F_N^{(1)}$, $F_N^{(2)}, \ldots, N > 2$, in order to keep (2.16) and (2.17) asymptotically uniform for times $\omega_{k_0} t = \mathrm{O}(\epsilon^{-2})$. Eqs. (2.18) and (2.19) describe the long time behavior of the system.

This method goes by many names, averaging, multiple timescales, etc., familiar to nonlinear physicists (see, e.g., [3,19–21]). It will turn out that $F_2^{(2)}$ depends only on n_k itself leading to a closed equation for the particle number, the QKE. It will also turn out that $F_N^{(1)}$, $F_N^{(2)}$, $N > 2$, are simply products of $Q_N^{(0)}$ with a function of n_k, which is the symmetric sum of N components. This means that the resulting equations (2.19) are easily solved by simply renormalizing the frequency.

The quantum kinetic equation is given by

$$\frac{\partial}{\partial t} n_k \equiv \epsilon^2 F_2^{(2)} = \left(4\epsilon^2 \int |T_{01',2'3'}|^2 \delta^{01'}_{2'3'} \, \mathrm{d}1'2'3' \times (\pi \, \mathrm{sgn}(t) \delta(\tilde{\Delta}^{01'}_{2'3'})) \right.$$

$$\left. \times (n_{2'} n_{3'} (1 - n_{1'} - n_k) + n_k n_{1'} (n_{2'} + n_{3'} - 1)) \right), \tag{2.20}$$

where the Hartree–Fock self-energy is

$$\tilde{\Delta}^{1'2'}_{3'4'} = \omega_{1'} + \omega_{2'} - \omega_{3'} - \omega_{4'} + 2 \int \mathrm{d}1((T_{1'1,11'} + T_{2'1,12'} - T_{3'1,13'} - T_{4'1,14'}) n_1).$$

From the form of (2.20), it is clear that number density is redistributed by binary particle collisions which satisfy momentum and energy conservation. In particular, exchange of particle number (momenta, energy) is associated with particles whose momenta and energies lie on the resonant manifold defined to a good approximation by

$$\mathbf{k}_1 + \mathbf{k}_2 - \mathbf{k}_3 - \mathbf{k}_4 = 0, \qquad \omega_{k_1} + \omega_{k_2} - \omega_{k_3} - \omega_{k_4} = 0. \tag{2.21}$$

The evolution equation for $Q^{(0)}_{1'2',\ldots,N}$ can be written

$$\frac{\partial \ln Q^{(0)}_{12,\ldots,N}}{\partial t} = \mathrm{i}\left(\sum_{i=1}^{N/2}\Omega_i - \sum_{i=N/2+1}^{N}\Omega_i^*\right),$$

$$\Omega_{k'} = \omega_{k'} + 2\epsilon\int \mathrm{d}1\, n_1 T_{1'1,11'} + 2\epsilon^2\int \mathrm{d}123\,(n_1 + n_2 n_3 - n_1 n_3 - n_1 n_2)\,|T_{k'123}|^2\delta^{k'1}_{23}$$

$$\times\left(P\left(\frac{1}{\tilde{\Delta}^{k'1}_{23}}\right) + \mathrm{i}\pi\,\mathrm{sgn}(t)\delta(\tilde{\Delta}^{k'1}_{23})\right), \tag{2.22}$$

which can be interpreted as a complex frequency renormalization.

We can calculate the sign of $\mathrm{Im}\,\Omega$ once n_k reaches its steady (equilibrium) state. For steady state $\dot{n}_k = 0$ we rewrite the QKE (2.20) as [3]

$$\int |T_{01',2'3'}|^2\delta^{01'}_{2'3'}\,\mathrm{d}1'2'3' \times (\pi\,\mathrm{sgn}(t)\delta(\tilde{\Delta}^{01'}_{2'3'}))(n_{2'}n_{3'} - n_{1'}n_{2'} - n_{1'}n_{3'} + n_{1'})$$

$$= \frac{1}{n_k}\int |T_{01',2'3'}|^2\delta^{01'}_{2'3'}\,\mathrm{d}1'2'3' \times (\pi\,\mathrm{sgn}(t)\delta(\tilde{\Delta}^{01'}_{2'3'}))(n_{2'}n_{3'}(1 - n_{1'})) \geq 0. \tag{2.23}$$

The left-hand side of the above equation is the imaginary part of Ω_k. Observe that, because $\mathrm{Im}\,\Omega_k \geq 0$, the leading order approximation to the Nth ($N \geq 2$) order cumulant decays with time. This means that the memory of (smooth) initial states is gradually forgotten.

We want to make two very important points which are often overlooked. While the leading order contributions (which at $t = 0$ is the initial state multiplied by an oscillatory factor) to the Nth order cumulants for $N > 2$ play no role in the long time behavior of the system and indeed slowly decay, higher order (in ϵ) contributions do not disappear in the long time limit. The system retains a weakly non-Gaussian character which is responsible and essential for particle number and energy transfer. For example, in the long time limit, the order ϵ fourth order cumulant has the quasi-stationary contribution (the terms with higher order cumulants asymptote to zero by means of phase mixing and the Riemann–Lebesgue lemma)

$$\mathcal{P}^{(1)}_{1'2'3'4'}(t) = 2\mathrm{i}T_{4'3',2'1'}(n_{3'}n_{4'}(1 - n_{2'} - n_{1'}) + n_{1'}n_{2'}(n_{3'} + n_{4'} - 1)) \times A_t(\tilde{\Delta}^{1'2'}_{3'4'}), \tag{2.24}$$

where

$$A_t(x) = \int_0^t \mathrm{d}\tau\,\exp[\mathrm{i}x\tau].$$

Because $\lim_{t\to\infty} A_t(x) = \pi\,\mathrm{sgn}\,t\cdot\delta(x) + \mathrm{i}P(1/x)$, in the limit $t \to \infty$,

$$\mathcal{P}^{(1)}_{1'2'3'4'}(t) \to 2\mathrm{i}T_{4'3',2'1'}(n_{3'}n_{4'}(1 - n_{2'} - n_{1'}) + n_{1'}n_{2'}(n_{3'} + n_{4'} - 1))\left(\pi\,\mathrm{sgn}\,t\cdot\delta(\tilde{\Delta}^{1'2'}_{3'4'}) + \mathrm{i}P\left(\frac{1}{\tilde{\Delta}^{1'2'}_{3'4'}}\right)\right).$$

Thus, in the long time limit, the order ϵ contribution $\mathcal{P}^{(1)}_{1234}$ to the fourth order cumulant is not smooth but is given by a sum of generalized functions represented by the Dirac delta function and the Cauchy principal value. We may therefore legitimately ask: in what sense is the asymptotic series (2.16) and (2.17) well-ordered if it contains terms which are products of powers of ϵ with generalized functions? The answer is that to analyze properly the asymptotic

[3] Recall that $\phi \leq n_k \leq 1$ as a manifestation of Pauli exclusion principle.

behavior of the system, we must always revert to physical space and look at the corresponding asymptotic expansion for the cumulants $\{\psi^\dagger(\mathbf{r})\psi^\dagger(\mathbf{r}')\psi(\mathbf{r}'')\psi(\mathbf{r}''')\}$ connected with fourth order expectation values of the field operators. These objects, which decay to zero as the separations $\mathbf{r}'-\mathbf{r}$, $\mathbf{r}''-\mathbf{r}$, $\mathbf{r}'''-\mathbf{r}$ tend to infinity, are simply the Fourier transform of $\mathcal{P}_{kk'k''k'''}$. We can also show that no terms worse than single delta functions occur (or products of delta functions which have their support on different resonant submanifolds) at later powers of ϵ so that the resulting asymptotic expansion for the spatial cumulants is indeed well ordered.

The second important point concerns the reversibility or rather the retraceability of solutions of (2.20) and (2.22). In the derivation of (2.20) and (2.22), we assumed that the initial cumulants were sufficiently smooth so that integrals over momentum space of multiplications of the initial values of Q_N by $\exp(-\mathrm{i}(\omega_1+\cdots-\omega_N)t)$ tend to zero in the asymptotic limit. However, it is clear from (2.22) that the regenerated cumulants have terms of higher order in ϵ which are not smooth and indeed have their (singular) support precisely on the resonant manifold which is the exponent of the oscillatory exponential. What would happen, then, if one were to redo the initial value problem from a later time $t_1 = \mathrm{O}(\epsilon^{-2})$, either positive or negative, after which the fourth order cumulant had developed a non-smooth part? On the surface, it would seem that the sgn term in (2.22) would be $\mathrm{sgn}(t-t_1)$ so that, at every time t_1, there would be a discontinuity in the slope of $n_k(t)$. But that is not the case. If one accounts for the non-smooth behavior (2.22) in the new initial value for $\mathcal{P}^{(1)}_{1234}$, then one gets additional terms in (2.22) which give exactly the same collision integral but with the factor $(\mathrm{sgn}\, t - \mathrm{sgn}(t-t_1))$. Adding the two contributions, we find that the QKE is exactly the same as the one derived in the beginning at $t=0$. It is not that the point $t=0$ is so special. Rather, there is a range of times t, $-\epsilon^{-2} \ll \omega_{k_0} t \ll \epsilon^{-2}$, such that, if one begins anywhere within this range, an initially smooth distribution stays smooth. But once the limit $t \to \infty$, $\epsilon^2 t$ finite, is taken, an irreversibility and non-smoothness in the cumulants is introduced.

In a very real sense, then, the infinite-dimensional Hamiltonian system acts as if there is an attracting manifold (an inertial or generalized center manifold in the modern vernacular) in its phase space to which the system relaxes as $\omega_{k_0} t \to \mathrm{O}(\epsilon^{-2})$ (in either time direction) on which the slow dynamics is given by the closure equations (2.20) and (2.22). On this attracting manifold, the higher order cumulants are essentially slaved to the particle number density and their frequencies are renormalized by contributions which also depend on particle number density. The attenuation in this case is due to losses to the heat bath consisting of all momenta which do not lie on a resonance manifold associated with $\mathbf{k}$.

3. Analysis of the kinetic equation

3.1. Conservation laws, thermodynamic and finite-flux solutions of the kinetic equation

The collision integral in (2.20) has the following constants of motion:

$$\mathcal{N} = \frac{V}{(2\pi)^d}\int \mathbf{dk}\, n_k, \quad \mathbf{P} = \frac{V}{(2\pi)^d}\int \hbar\mathbf{k}\, \mathbf{dk}\, n_k, \quad \mathcal{E} = \frac{V}{(2\pi)^d}\int \frac{\hbar^2|\vec{k}|^2}{2m}\mathbf{dk}\, n_k, \tag{3.1}$$

which can be identified as number of particles, momentum and kinetic energy. In spatially homogeneous systems, $\mathbf{P}=0$ so that the only relevant constants of motion are $\mathcal{N}$ and $\mathcal{E}$.

In this article we will be dealing with the isotropic case only, and for simplicity, neglect the spin degree of freedom. Therefore, we simplify the collision integral by averaging it over all angles. First, we change variables from particle momentum $\mathbf{k}$ to the particle kinetic energy

$$\epsilon_k = \hbar\omega_k = \frac{\hbar^2 k^2}{2m}, \tag{3.2}$$

where m is the coefficient of proportionality between ω_k and $\hbar k^2/2$, and can be associated with (effective) mass of the interacting particles.

We introduce $n_\omega = n(\mathbf{k}(\omega))$ and rewrite the kinetic equation as

$$\dot{n}_\omega = \frac{1}{\Omega_0 k^{d-1}(\mathrm{d}k/\mathrm{d}\omega)} \int \int_{\omega_i>0, i=1,2,3} \int \mathcal{K}(\omega, \omega_1, \omega_2, \omega_3) S_{\omega\omega_1\omega_2\omega_3} \times \delta(\omega + \omega_1 - \omega_2 - \omega_3) \mathrm{d}\omega_1 \, \mathrm{d}\omega_2 \, \mathrm{d}\omega_3, \tag{3.3}$$

where $S_{\omega\omega_1\omega_2\omega_3}$ is the angle-averaged potential,

$$S_{\omega\omega_1\omega_2\omega_3} = 4\pi \Omega_0 (k k_1 k_2 k_3)^{(d-1)} \frac{\mathrm{d}k}{\mathrm{d}\omega} \frac{\mathrm{d}k_1}{\mathrm{d}\omega_1} \frac{\mathrm{d}k_2}{\mathrm{d}\omega_2} \frac{\mathrm{d}k_3}{\mathrm{d}\omega_3} \cdot \langle |T_{kk_1,k_2k_3}|^2 \delta(\mathbf{k} + \mathbf{k_1} - \mathbf{k_2} - \mathbf{k_3}) \rangle. \tag{3.4}$$

The brackets $\langle \cdot \rangle$ denote averages over unit spheres (including the $V/(2\pi)^d$ factors) in $\mathbf{k}, \mathbf{k}_1, \mathbf{k}_2, \mathbf{k}_3$ space (i.e., we have integrated over all angular contributions) and Ω_0 is the surface area of the unit sphere in d dimensions. Although in our case $d = 3$, we want to stress that with the above notation the results can easily be extended to other dimensions, e.g., to $d = 2$ which is appropriate for the description of semiconductor quantum wells. $\mathcal{K}$ is the kernel of kinetic equation, which for the quantum (fermionic), quantum (bosonic) and classical cases is given, respectively, by:

$$\begin{aligned}
\mathcal{K}^{\text{fermionic}}(\omega, \omega_1, \omega_2, \omega_3) &= n_{\omega_2} n_{\omega_3} (1 - n_{\omega_1})(1 - n_\omega) - n_\omega n_{\omega_1} (1 - n_{\omega_2})(1 - n_{\omega_3}), \\
\mathcal{K}^{\text{bosonic}}(\omega, \omega_1, \omega_2, \omega_3) &= (n_{\omega_2} n_{\omega_3} (n_\omega + n_{\omega_1} + 1) - n_\omega n_{\omega_1} (n_{\omega_2} + n_{\omega_3} + 1)), \\
\mathcal{K}^{\text{classical}}(\omega, \omega_1, \omega_2, \omega_3) &= (n_{\omega_2} n_{\omega_3} (n_\omega + n_{\omega_1}) - n_\omega n_{\omega_1} (n_{\omega_2} + n_{\omega_3})).
\end{aligned} \tag{3.5}$$

We then introduce the particle density per frequency

$$N_\omega = \Omega_0 k^{d-1} (\mathrm{d}k/\mathrm{d}\omega) n_\omega$$

so that $\int N_\omega \, \mathrm{d}\omega = \int n_k \, \mathbf{dk}$ and

$$\dot{N}_\omega = \int_{\omega_1,\omega_2,\omega_3>0} \int \int \mathcal{K}(\omega, \omega_1, \omega_2, \omega_3) S_{\omega\omega_1\omega_2\omega_3} \delta(\omega + \omega_1 - \omega_2 - \omega_3) \, \mathrm{d}\omega_1 \, \mathrm{d}\omega_2 \, \mathrm{d}\omega_3. \tag{3.6}$$

One class of steady (equilibrium) solutions of the KE corresponds to the thermal equilibrium. For fermionic systems, it is given by the Fermi–Dirac (FD) distribution, and for bosonic systems it is given by the Bose–Einstein distribution,

$$n_k = \frac{1}{\exp(\beta(\epsilon_k - \mu)) \pm 1}, \tag{3.7}$$

where the plus sign corresponds to the fermion case and the minus sign to the bosonic case. μ is the chemical potential and β is the inverse temperature in energy units. The classical analog of the quantum thermal equilibrium distribution is given by the Rayleigh–Jeans distribution

$$n(k) = T/(\mu + \epsilon_k). \tag{3.8}$$

It is easy to check that the solutions (3.7) and (3.8) make the integrand in (3.3) and (3.6) exactly zero in all three cases.

However, the thermodynamic equilibrium is not the most general steady (equilibrium) solution of the kinetic equation and indeed in some cases has little relevance. The solutions we are most interested in are those which

describe the steady state reached *between* ranges of frequencies where particles and energy are added to or removed from the system. These regions, where there is no pumping or dumping, are called "windows of transparency" or "inertial ranges". In particular, we have in mind the following situation. Particles and energy are added to the system in a narrow range of intermediate frequencies about ω_0. Particles and energy are drained from the system in a range of frequencies about $\omega < \omega_L < \omega_0$ and for $\omega > \omega_R > \omega_0$. Because of conservation of energy and particles in the inertial ranges between ω_L and ω_0 and between ω_0 and ω_R, where there is no pumping or damping and because the relations between particle number N_ω and energy density $E_\omega = \omega N_\omega$, we will find that a net flux of energy to the higher frequencies must be accompanied by a net flux of particles to lower frequencies as it might be expected by analogy with classical wave turbulence. The presence of sources and sinks drives the system away from the thermodynamic equilibrium. Therefore, in the windows of transparency, $\omega_L < \omega < \omega_0$ and $\omega_0 < \omega < \omega_R$, the system can also relax to equilibrium distributions corresponding to a finite flux of particles and energy flowing through these windows from the sources to the sinks. These are the new solutions of the QKE. The number of such finite flux solutions corresponds to the number of conserved densities (here two, n_k and $\omega_k n_k$, or N_ω and ωN_ω) of the QKE.

To demonstrate the existence of such solutions, we rewrite the KE in the following form:

$$\begin{aligned} \dot{N}_\omega &= \frac{\partial^2}{\partial\omega^2}\mathcal{W}[n_\omega], \\ \mathcal{W}[n_\omega] &= \int\int\int_{\Omega} (\omega + \omega_1 - \omega_2 - \omega_3)\mathcal{K}_{\omega_2+\omega_3-\omega,\omega_2,\omega_3} S_{\omega_2+\omega_3-\omega,\omega_2,\omega_3}\, \mathrm{d}\omega_1\, \mathrm{d}\omega_2\, \mathrm{d}\omega_3, \end{aligned} \tag{3.9}$$

where the integration is over the region $\Omega\{\omega_1, \omega_2, \omega_3 > 0, \quad \omega_1 < \omega_2 + \omega_3 < \omega + \omega_1\}$. This expression can be checked by direct differentiation.

The relevant kinetic equation, which includes the presence of sources and sinks, is

$$\frac{\partial N_\omega}{\partial t} = \frac{\partial^2}{\partial\omega^2}\mathcal{W}[n_\omega] + F_\omega - D_\omega, \tag{3.10}$$

where we think of F_ω as having its support near $\omega = \omega_0$ and D_ω its support below ω_L and above ω_R. We ask if (3.10) leads to a steady (equilibrium) solutions in the transparency regions $\omega_L < \omega < \omega_0$ and $\omega_0 < \omega < \omega_R$, where $F_\omega = D_\omega = 0$ corresponding to a finite flux of particles and energy across these windows. One can readily associate the quantities

$$Q = \frac{\partial\mathcal{W}}{\partial\omega}, \qquad \frac{\partial N_\omega}{\partial t} = \frac{\partial Q}{\partial\omega}$$

and

$$P = \mathcal{W} - \omega\frac{\partial\mathcal{W}}{\partial\omega}, \qquad \frac{\partial\omega N_\omega}{\partial t} = -\frac{\partial P}{\partial\omega}, \tag{3.11}$$

with the fluxes P and Q of particles N_ω and energy $E_\omega = \omega N_\omega$. Q and P are taken to be positive if they flow leftward and rightward, respectively. In the windows of transparency, we look for solutions for which N_ω is constant in time and then (3.9) integrates to

$$\mathcal{W} = Q\omega + P, \tag{3.12}$$

where Q and P are constants. The two-parameter family of thermodynamic solutions, parametrized by T and μ, is given by solving the homogeneous equation $\mathcal{W} = 0$ for which $P = Q = 0$. Therefore, the thermodynamic

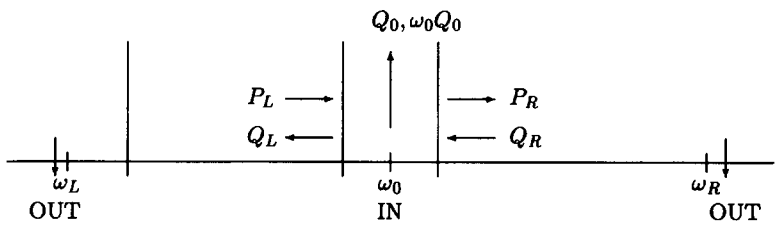

Fig. 1. The setup for input–output fluxes. Carriers and energy are added at ω_0 at rates Q_0 and $\omega_0 Q_0$, respectively. Energy and some carriers are dissipated at $\omega_R > \omega_0$ (an idealization) and carriers and some energy are absorbed by the laser at ω_L. Finite flux stationary solutions are realized in the windows (ω_L, ω_0) and (ω_0, ω_R) although in practice there will be some losses through both these regions.

solutions carry no fluxes of particles or energy. A more general[4] steady (equilibrium) solution to (3.9) therefore is the four-parameter family

$$n_\omega = n_\omega(T, \mu, P, Q). \tag{3.13}$$

We are particularly interested in the solutions for which Q_0 particles per unit time and $\omega_0 Q_0$ units of energy per unit time are fed to the system in a narrow frequency window about $\omega = \omega_0$. We will assume that the flux of particles passing through the left (right) window $\omega_L < \omega < \omega_0$ $(\omega_0 < \omega < \omega_R)$ is Q_L (Q_R) and the flux of energy through the right (left) window is P_R (P_L). We will also assume that the sinks consume all the particles and energy that reach them. Then (see Fig. 1)

$$Q_L - Q_R = Q_0, \qquad P_R - P_L = \omega_0 Q_0, \qquad P_L = -\omega_L Q_L, \qquad Q_R = -\frac{1}{\omega_R} P_R. \tag{3.14}$$

The first two relations in (3.14) express conservation of particles and energy. The second two express the fact that, in order to maintain equilibrium, the rate of particle destruction at ω_R is the rate of energy destroyed there divided by the energy per particle. Likewise the amount of energy destroyed at ω_L (which absorption, in the context of application discussed in Section 5, will be due to semiconductor lasing) must be ω_L times the number of particles absorbed there. Solving (3.14) we obtain

$$\begin{aligned} Q_L &= Q_0(\omega_R - \omega_0)/(\omega_R - \omega_L), \qquad & Q_R &= -Q_0(\omega_0 - \omega_L)/(\omega_R - \omega_L), \\ P_R &= Q_0\omega_R(\omega_0 - \omega_L)/(\omega_R - \omega_L), \qquad & P_L &= -\omega_L Q_0(\omega_R - \omega_0)/(\omega_R - \omega_L). \end{aligned} \tag{3.15}$$

We see that for $\omega_L \ll \omega_0 \ll \omega_R$, $|Q_R| \ll Q_L \simeq Q_0$, $|P_L| \ll P_R \simeq \omega_0 Q_0$ so that the solutions are almost pure Kolmogorov in the sense that almost all energy flows to ω_R and almost all particles flow to ω_L. However, it is important to stress that in the left-window, (3.12) becomes

$$\mathcal{W} = Q_L(\omega - \omega_L) \tag{3.16}$$

and in the right-window

$$\mathcal{W} = P_R\left(1 - \frac{\omega}{\omega_R}\right) \tag{3.17}$$

[4] On purpose we do not say "the most general solutions", as there may be some hidden symmetries of the QKE which generate more conserved quantities and thus more general solutions, corresponding to fluxes of those quantities. The statement that the general KE with M conserved quantities has "a most general solution" depending on $2M$ parameters is also not proven yet for the general collision integral. Remember also that we are considering the isotropic case. This is, of course, an idealization, and generally "drift" solutions may be of equal importance.

so that the right-hand sides vanish if the frequency approaches the sink value. This aids convergence in these windows.

Solutions to (3.16) and (3.17) have not been investigated even in the classical case. In the classical case, Zakharov (see, e.g., [22,23]) had found the pure Kolmogorov solutions $T = \mu = P = 0$, $T = \mu = Q = 0$ which turn out to have power law behavior $n_\omega = c\omega^{-x}$. Likewise, in the bosonic case, several authors have attempted to find power law solutions which essentially balance the quadratic terms in $\mathcal{W}^{\text{bosonic}}$ with a finite energy flux. However, in the differential approximation for neither bosons nor fermions are there power law solutions.

In many cases it may be that whenever $\omega_R \gg \omega_0$, ω_L may not be all that much smaller than ω_0. We return to this application after introducing an enormous simplification for $\mathcal{W}$ which gives a very good qualitative description of the collision integral.

4. Differential kinetic equation

4.1. Derivation of differential quantum kinetic equation

To simplify our analysis, we use an approximation to the kinetic equation known as the differential approximation (see, e.g., [16–18]). The differential quantum kinetic equation (DQKE) gives qualitatively correct behavior in general, but is strictly valid only when the particle and energy transfer happens primarily between neighbors in momentum space. It is easy to verify that it has a four-parameter family of a steady (equilibrium) solutions and it is easy to identify two of these parameters as the flux of particle number and energy, respectively, and the other two as temperature and chemical potential. The analytical expressions for the fluxes can be calculated so that, for any given distribution, the corresponding fluxes may be easily computed numerically. The steady (equilibrium) solutions can be found analytically in various limits. The DQKE is much more suitable for numerical experiments than the full collision integral, simply because it is easier and faster to compute derivatives than integrals of the collision type.

We now demonstrate the derivation of the differential approximation in the fermion case. This result is new. The results for the cases of classical waves and bosonic systems are given in (4.9). Assume that $S_{\omega\omega_1\omega_2\omega_3}$ is dominated by its contribution from the region $\omega \simeq \omega_1 \simeq \omega_2 \simeq \omega_3$. We call such a coupling coefficient "strongly diagonal". Then obviously the integrand of the QKE deviates significantly from zero in the same region. The first derivation of the differential kinetic equation proceeds as follows [28]. Multiply both sides of (3.6) by a sufficiently smooth function $\Phi(\omega)$ and integrate with respect to ω:

$$\int \dot{N}_\omega \Phi(\omega)\,\mathrm{d}\omega = \int\int\int \mathcal{K}(\omega,\omega_1,\omega_2,\omega_3) \times S_{\omega,\omega_1,\omega_2,\omega_3}\delta(\omega+\omega_1-\omega_2-\omega_3)\Phi(\omega)\,\mathrm{d}\omega\,\mathrm{d}\omega_1\,\mathrm{d}\omega_2\,\mathrm{d}\omega_3. \tag{4.1}$$

Symmetrize the right-hand side of Eq. (4.1) to get

$$\int \dot{N}_\omega \Phi(\omega)\mathrm{d}\omega = \int\int\int \mathcal{K}(\omega,\omega_1,\omega_2,\omega_3) S_{\omega,\omega_1,\omega_2,\omega_3}\delta(\omega+\omega_1-\omega_2-\omega_3) \times \tfrac{1}{4}(\Phi(\omega)+\Phi(\omega_1)-\Phi(\omega_2)-\Phi(\omega_3))\,\mathrm{d}\omega\,\mathrm{d}\omega_1\,\mathrm{d}\omega_2\,\mathrm{d}\omega_3. \tag{4.2}$$

To do this we use the symmetries of the kernel of collision integral responsible for particle number and energy conservation. Without this symmetrization the resulting kinetic equation would not conserve particle number and energy. Now make a change of variables $\omega_i = \omega + \Delta_i$, $i = 1, 2, 3$, and expand Φ in the Taylor series with respect to Δ_i around ω. The first non-zero term in the expansion contains the second derivative $\Phi''(\omega)$:

$$\Phi(\omega) + \Phi(\omega + \Delta_1) - \Phi(\omega + \Delta_2) - \Phi(\omega + \Delta_1 - \Delta_2) = (\Delta_1 - \Delta_2)\Delta_2\Phi''(\omega) + \mathrm{O}(\Delta^2). \tag{4.3}$$

We also expand $n_{\omega_i} = n_\omega + \Delta_i n'_\omega + \Delta_i^2/2 n''_\omega$ in the kernel $\mathcal{K}^{\text{fermionic}}(\omega, \omega_1, \omega_2, \omega_3)$ of the kinetic equation,

$$\begin{aligned}&\mathcal{K}^{\text{fermionic}}(\omega, \omega + \Delta_1, \omega + \Delta_2, \omega + \Delta_1 - \Delta_2)\\ &\quad = (\Delta_1 - \Delta_2)\Delta_2(n'^2_\omega(1 - 2n_\omega) + n_\omega n''_\omega(n_\omega - 1)).\end{aligned} \tag{4.4}$$

We then substitute (4.3) and (4.4) in (4.2), integrate twice by parts the $\Phi''(\omega)$ term to get

$$\begin{aligned}&\int \mathrm{d}\omega\, \Phi(\omega)\left[\dot{N}_\omega - \frac{\partial^2}{\partial\omega^2}(n'^2_\omega(1 - 2n_\omega) + n_\omega n''_\omega(n_\omega - 1))\right.\\ &\left.\quad \times \int \mathrm{d}\Delta_1\, \mathrm{d}\Delta_2\, S_{\omega,\omega+\Delta_1,\omega+\Delta_2,\omega+\Delta_1-\Delta_2}(\Delta_2(\Delta_1 - \Delta_2))^2\right] = 0.\end{aligned} \tag{4.5}$$

Using the arbitrariness of Φ we finally get

$$\begin{aligned}\dot{n}_\omega = &-\frac{1}{\Omega_0 k^{d-1}(\mathrm{d}k/\mathrm{d}\omega)}\frac{1}{4}\frac{\partial^2}{\partial\omega^2}\left[\left(n^4_\omega\frac{\partial^2}{\partial\omega^2}\left(\frac{1}{n_\omega}\right) + n^2_\omega\frac{\partial^2}{\partial\omega^2}(\ln(n_\omega))\right)\right.\\ &\left.\times \int \mathrm{d}\Delta_1\, \mathrm{d}\Delta_2\, S_{\omega,\omega+\Delta_1,\omega+\Delta_2,\omega+\Delta_1-\Delta_2}(\Delta_2(\Delta_1 - \Delta_2))^2\right].\end{aligned}$$

Finally, we assume that $S_{\omega\omega_1\omega_2\omega_3}$ is a homogeneous function of its arguments of degree γ:

$$S_{\epsilon\omega,\epsilon\omega_1,\epsilon\omega_2,\epsilon\omega_3} = \epsilon^\gamma S_{\omega\omega_1\omega_2\omega_3}. \tag{4.6}$$

We define $\omega\delta_i = \Delta_i$, and rewrite the DQKE as

$$\dot{n}_\omega = -\frac{1}{\Omega_0 k^{d-1}(\mathrm{d}k/\mathrm{d}\omega)}\frac{\partial^2}{\partial\omega^2}\left[\left(n^4_\omega\frac{\partial^2}{\partial\omega^2}\left(\frac{1}{n_\omega}\right) + n^2_\omega\frac{\partial^2}{\partial\omega^2}(\ln(n_\omega))\right) \times I \times \omega^s\right], \tag{4.7}$$

where I is the interaction strength,

$$I = \frac{1}{4}\int \mathrm{d}\delta_1\, \mathrm{d}\delta_2\, S_{1,1+\delta_1,1+\delta_2,1+\delta_1-\delta_2}(\delta_2(\delta_1 - \delta_2))^2,$$

and $s = \gamma + 6$.

An alternative derivation of the DQKE can be given by applying the Zakharov transformation (see, e.g., [23]) directly to the QKE. The Zakharov transformation is a conformal change of variables which reveals the symmetry of original collision integral. It transforms certain regions of the integration domain, and in the classical case, makes the transformed collision integral have a zero integrand for certain power law distributions. The Zakharov-transformed KE takes the form

$$\begin{aligned}\dot{n}_\omega = &\frac{1}{\Omega_0 k^{d-1}(\mathrm{d}k/\mathrm{d}\omega)} \times \frac{1}{4} \times \int_{\Delta_1}\int\left(\mathcal{K}(\omega, \omega_1, \omega_2, \omega_3) + \left(\frac{\omega}{\omega_2}\right)^{\gamma+3}\mathcal{K}\left(\omega, \frac{\omega\omega_3}{\omega_2}, \frac{\omega^2}{\omega_2}, \frac{\omega\omega_1}{\omega_2}\right)\right.\\ &+ \left(\frac{\omega}{\omega_1}\right)^{\gamma+3}\mathcal{K}\left(\omega, \frac{\omega^2}{\omega_1}, \frac{\omega\omega_2}{\omega_1}, \frac{\omega\omega_3}{\omega_1}\right) + \left(\frac{\omega}{\omega_3}\right)^{\gamma+3}\mathcal{K}\left(\omega, \frac{\omega\omega_2}{\omega_3}, \frac{\omega\omega_1}{\omega_3}, \frac{\omega^2}{\omega_3}\right)\Bigg)\\ &\times S_{\omega\omega_1\omega_2\omega_3}\delta(\omega + \omega_1 - \omega_2 - \omega_3)\,\mathrm{d}\omega_1\,\mathrm{d}\omega_2\,\mathrm{d}\omega_3.\end{aligned} \tag{4.8}$$

We then expand the right-hand side of the above equation in powers of Δ's. The first non-vanishing term is of order Δ^4 and can be represented as second order derivative with respect to ω of $[(n^4_\omega(\partial^2/\partial\omega^2)(1/n_\omega) + n^2_\omega(\partial^2/\partial\omega^2)(\ln(n_\omega))) \times I \times \omega^s]$. The resulting DQKE is given in (4.7).

4.2. Solutions and properties of the DQKE

Let us now rewrite the DQKE in the form:

$$\begin{aligned}
&\dot{N}_\omega = \frac{\partial^2}{\partial\omega^2}\mathcal{W}[n_\omega],\\
&\mathcal{W}^{\text{fermionic}}[n_\omega] = -I\left(n_\omega^4\frac{\partial^2}{\partial\omega^2}\left(\frac{1}{n_\omega}\right) + n_\omega^2\frac{\partial^2}{\partial\omega^2}(\ln(n_\omega))\right)\times\omega^s,\\
&\mathcal{W}^{\text{bosonic}}[n_\omega] = I\left(n_\omega^4\frac{\partial^2}{\partial\omega^2}\left(\frac{1}{n_\omega}\right) - n_\omega^2\frac{\partial^2}{\partial\omega^2}(\ln(n_\omega))\right)\times\omega^s,\\
&\mathcal{W}^{\text{classical}}[n_\omega] = I\left(n_\omega^4\frac{\partial^2}{\partial\omega^2}\left(\frac{1}{n_\omega}\right)\right)\times\omega^s.
\end{aligned} \tag{4.9}$$

We can now use (3.11) to calculate the fluxes P and Q in terms of n_ω and its derivatives. We concentrate on the fermionic case. There,

$$\begin{aligned}
Q &= \frac{\partial\mathcal{W}}{\partial\omega} = Is\omega^{s-1}(-n'^2(2n-1) - nn''(1-n)) + I\omega^s(-2n'^3 + n'n''(1-2n) + nn'''(n-1)),\\
P &= \left(\mathcal{W} - \omega\frac{\partial\mathcal{W}}{\partial\omega}\right) = I\omega^s(1-s)(-n'^2(2n-1) - nn''(1-n))\\
&\quad - I\omega^{s+1}(-2n'^3 + n'n''(1-2n) + nn'''(n-1)).
\end{aligned} \tag{4.10}$$

Let us make a change of variables $n = 1/(G+1)$ and $n = 1/(\mathrm{e}^m + 1)$. n, G, m are functions of ω and t, "dot" is used to denote differentiation with respect to time, and "prime" with respect to ω. Then

$$\dot{G} = (1+G)^2\frac{I}{\Omega_0 k^{d-1}(\mathrm{d}k/\mathrm{d}\omega)}\frac{\partial^2}{\partial\omega^2}\left(\omega^s\frac{G'^2 - GG''}{(1+G)^4}\right)$$

or

$$\dot{m}_\omega = -\frac{I}{\Omega_0 k^{d-1}(\mathrm{d}k/\mathrm{d}\omega)}\cosh^2\left(\frac{m}{2}\right)\frac{\partial^2}{\partial\omega^2}\omega^s\frac{m''}{4\cosh^4(m/2)}. \tag{4.11}$$

Since the stationary DQKE is a fourth order ODE, its solutions will have four free parameters. Indeed, assume a steady (equilibrium) state and integrate (4.9) and (4.11) twice to get

$$\mathcal{W}[n_\omega] = Q\omega + P,$$

or

$$G = \exp\left(-\frac{\partial^{-2}}{\partial\omega^2}\frac{(Q\omega+P)(G+1)^4}{I\omega^s G^2}\right),$$

or

$$m'' = \frac{Q\omega+P}{I\omega^s}\cosh^4\left(\frac{m}{2}\right), \tag{4.12}$$

where Q and P are fluxes of particle number and energy. For $P = Q = 0$, (4.12) trivially gives

$$n(\omega) = \frac{1}{\exp[(\omega-\mu)/T]+1},$$

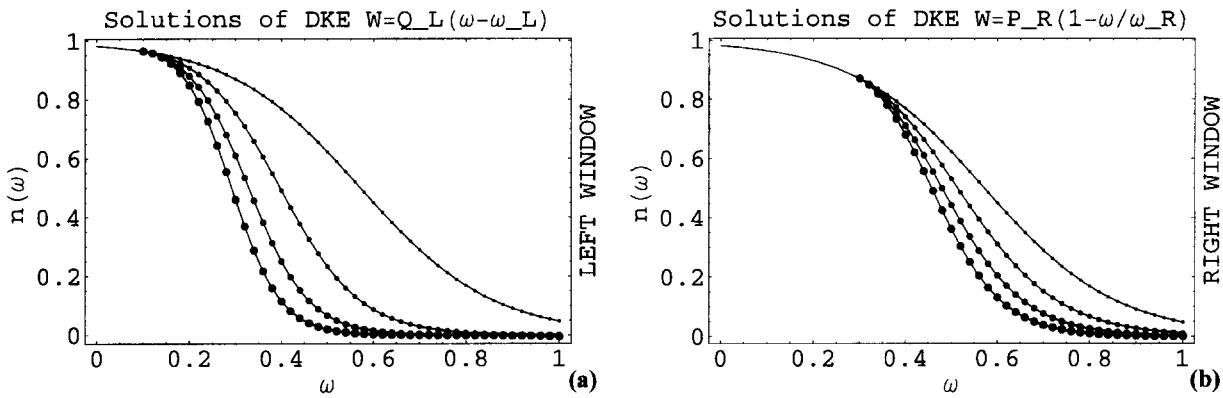

Fig. 2. (a) Numerical solution of (4.13). Initial conditions are $n_{\omega=0.1} = f_{\omega=0.1}$, $n'_{\omega=0.1} = f'_{\omega=0.1}$, where $f_\omega = 1/(\exp(7\omega - 4) + 1)$. The results are shown for $10^6 Q_L = 0, 3, 6, 9$. The dot size indicates the value of the flux, with larger dots corresponding to larger flux; (b) same as (a) but with (4.14) and $n_{\omega=0.3} = f_{\omega=0.3}$, $n'_{\omega=0.3} = f'_{\omega=0.3}$. The results are shown for $10^4 P_R = 0, 3, 6, 9$.

the Fermi–Dirac distribution function. Therefore we observe that the Fermi–Dirac distribution function corresponds to a zero flux solution of the kinetic equation, consistent with our findings of the previous section.

4.3. Numerical results

We now investigate numerically the DQKE to gain an intuitive understanding of its properties.

We begin by studying the time independent solutions of (4.9) and solve (3.16) as an initial value problem with $\mathcal{W}$ given by $\mathcal{W}^{\text{fermionic}}$ (see (4.9)),

$$Q_L(\omega - \omega_L) = \mathcal{W}^{\text{fermionic}} \equiv -I\left(n_\omega^4 \frac{\partial^2}{\partial\omega^2}\left(\frac{1}{n_\omega}\right) + n_\omega^2 \frac{\partial^2}{\partial\omega^2}(\ln(n_\omega))\right) \times \omega^s. \tag{4.13}$$

We start from $\omega = 0.1$ and take the initial conditions to be $n_{\omega=0.1} = f_{\omega=0.1}$, $n'_{\omega=0.1} = f'_{\omega=0.1}$, where f_ω is a conveniently chosen Fermi–Dirac distribution function $f_\omega = 1/(\exp(7\omega - 4) + 1)$. The results are shown in Fig. 2(a) for the range $10^6 Q_L = 0, 3, 6, 9$. For $Q_L = 0$ we recover the Fermi–Dirac distribution function f_ω. However, for non-zero Q the distribution deviates from the Fermi–Dirac function, and the bigger the flux, the bigger the deviation. For the same initial conditions, the graph of the number density n_ω for the positive finite flux distribution lies below that for the Fermi–Dirac distribution. Further, observe that, for the Fermi–Dirac solution, the chemical potential μ is simply the distance to the point of the inflection of n_ω and the temperature is the width of the exponential decay region. For finite positive fluxes, the distance to the point of inflection (which we call μ_Q) is less than $\mu_{Q=0} = \mu$. Likewise, T_Q, the width of the n_ω distribution for a finite flux is less than $T_0 = T$. As fluxes become larger, the finite flux equilibrium distribution becomes more and more like a Heavyside function with rapidly decreasing μ_Q. This means that n_ω is very small for all $\omega > \mu_Q$ and thus the system can be pumped in this region with little or no Pauli blocking. We exploit this in Section 5 where the application to semiconductor lasers is considered.

In semiconductor lasers, it is the finite temperature effect of broadening the Fermi–Dirac distribution that contributes to inefficiency. If one could operate at $T = 0$, then one could simply choose the chemical potential, related to the total carrier number (see, e.g., [24]), so that the distribution cuts off immediately after the lasing frequency. However, the finite temperature broadens the distribution and means that one has to pump momentum values which play no role in the lasing process. The effect of the finite flux is to make T effectively smaller.

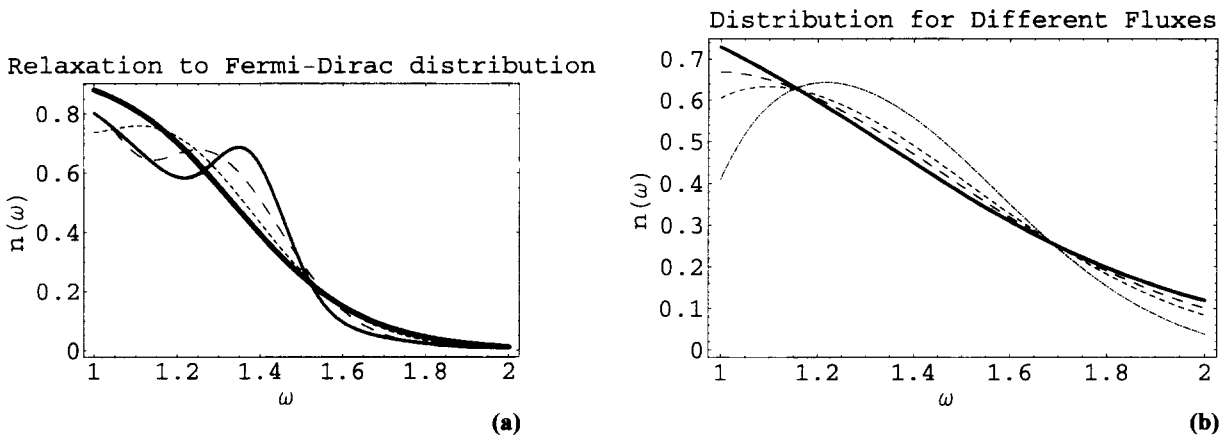

Fig. 3. (a) Time evolution of the distribution function as described by (4.9), with boundary conditions $P = Q = 0$ at both ends. The initial distribution (thin line) relaxes to a Fermi–Dirac state (thick line). Several intermediate states are shown by long-dashed and short-dashed lines; (b) same as (a), but for $P = 0$, $Q = Q_1 > Q_0$ at both ends. The initial distribution function (thick line) relaxes to finite-Q-equilibria as shown by the long-dashed line (only the final steady state is shown). Also shown are the results for the boundary conditions $P = 0$, $Q = Q_1 > Q_0$ at both ends (short-dashed line) and for $P = 0$, $Q = Q_2 > Q_1$ at both ends (dotted line).

We next solve (3.17) for the steady state solutions in the larger momentum region with $\mathcal{W}^{\text{fermionic}}$:

$$\mathcal{W} = P_{\text{R}}(1 - \omega/\omega_{\text{R}}) = \mathcal{W}^{\text{fermionic}} \equiv -I\left(n_\omega^4 \frac{\partial^2}{\partial\omega^2}\left(\frac{1}{n_\omega}\right) + n_\omega^2 \frac{\partial^2}{\partial\omega^2}(\ln(n_\omega))\right) \times \omega^s. \tag{4.14}$$

We start from $\omega = 0.3$ with initial conditions $n_{\omega=0.3} = f_{\omega=0.3}$, $n'_{\omega=0.3} = f'_{\omega=0.3}$. The results are shown in Fig. 2(b) for the range of $10^4 P_{\text{R}} = 0, 3, 6, 9$. Again, we recover the Fermi–Dirac function for zero flux, and observe a similar deviation from thermodynamical equilibrium for non-zero fluxes, namely the effective chemical potential and temperature diminishes with increasing of the flux value P_{R}.

We then consider the time evolution of the distribution function as given by the DQKE. The fundamental property of the kinetic equation that any distribution function relaxes to its thermodynamical equilibrium value in the absence of forcing (pumping/damping) is also true for the DQKE, as illustrated in Fig. 3(a). There an initial distribution function, shown by a thin solid line, relaxes to the FD function, shown by a thick solid line, through several intermediate states shown by dashed lines. Since there is no forcing to the system, we take "fluxless" boundary conditions $P = Q = 0$ in (4.11) on the boundaries, so that no particles or energy cross the boundaries. The distribution relaxes to the FD distribution roughly by the time τ_{relax}, which can be estimated as $\omega_{\text{max}}^{(2-s)}/(I(n+n^2))$, where ω_{max} is the frequency where distribution approaches zero value. To check that the final distribution is indeed FD, we calculate $\ln(1/n_\omega - 1)$ and verify that it is a linear function. The total particle number N and energy E are conserved in our numerical runs to an accuracy of 10^{-5}.

We then address the question of what is the steady (equilibrium) solution when the system has some external forcing. To model the forcing, we specify some positive flux of Q on the boundaries, and wait for the distribution to reach a new equilibrium, a hybrid state with a constant flux of Q, a zero P flux, energy E and particle number N (see, Fig. 3(b)). The more the flux of number of particles is, the more the final distribution is bent in the manner of Fig. 2 and according to (4.12). The total particle number N and energy E are the same for all curves on Fig. 3(b).

5. Application to semiconductor lasers

We will now investigate the relevance of finite flux solutions in the context of semiconductor lasers. In many ways, semiconductor lasers are similar to two level lasers in that the coherent light output is associated with the in-phase transitions of an electron from a higher to lower energy state. In semiconductors, the lower energy state is the valence band, from which sea electrons are removed leaving behind positively charged holes. The higher energy state is the conduction band. The quantum of energy released corresponds to an excited electron in the conduction band combining with a hole directly below (because the emitted photon has negligible momentum) in the lower band.

However, there are several important ways in which the semiconductor laser differs from and is more complicated than the traditional two-level laser model. First, in order for there to be lasing, there must be both an electron and hole available at the same momentum (and spin) value, whereas, in the traditional two-level laser, the ground state is always available for an excited electron. As a result, the excitation levels of both electrons and holes must be above a certain level. Second, there is a continuum of transition energies parametrized by the electron momentum $\mathbf{k}$, and the laser output is a weighted sum of contributions from polarizations corresponding to electron–hole pairs at each momentum value. In this feature, the semiconductor laser resembles an inhomogeneously broadened two-level laser. Third, electrons and holes interact with each other via Coulomb forces. Although this interaction is screened by the presence of many electrons and holes, it is nonetheless sufficiently strong to lead to a nonlinear coupling between electrons and holes at different momenta. It is this effect that gives rise to the coupling coefficient T_{kk_1,k_2k_3} of the earlier sections of this paper. The net effect of these collisions is a redistribution of carriers (the common name for both electrons and holes) across the momentum spectrum. In fact it is the fastest ($\approx$ 100 fs.) process (for electric field pulses of duration greater than picoseconds) and because of this, the gas of carriers essentially relaxes to a distribution corresponding to an equilibrium of this collision process. This equilibrium state is commonly taken to be that of thermodynamic equilibrium for fermion gases, the Fermi–Dirac distribution characterized by two parameters, the chemical potential μ and temperature T, slightly modified by the presence of broad-band pumping and damping. However, as we have shown, in situations where there is applied forcing and damping and in particular where these processes take place in separate regions of momentum space, the finite flux equilibria are more relevant.

In the semiconductor laser the applied forcing is usually the electrical pumping process. The low-energy sink is the actual lasing process, i.e., stimulated emission at the laser frequency. The high-energy sink has contributions from a variety of processes. One contribution is due to the fact that some of the charge carriers with high kinetic energies can leave the optically active region, and therefore, contribute to the electrial pumping current without contributing to the light amplification. Other processes acting as sinks are less well-localized at high energies. They are distributed over an extended range of momentum values. Examples are non-radiative recombination of electron–hole pairs mediated by impurities, dislocations, interface roughness, etc. In addition, Auger processes contribute significantly to the damping (i.e., loss) of charge carriers.

Although it is beyond the scope of this paper, we would like to mention that, for a complete description of relaxation and thermalization processes in semiconductor lasers, one would also have to take electron–phonon scattering into consideration. This interaction insures that the temperature of the electron–hole plasma is driven towards the lattice temperature. The main electron–phonon interactions involve longitudinal optical and acoustic phonons. The former couple via the Fröhlich interaction to the charge carriers and typical thermalization times are almost as short as those due to carrier–carrier interaction in semiconductor lasers (within a factor of about 5). Much slower (3–4 orders of magnitude) is the deformation potential coupling with acoustic phonons. Making the assumption that the electron–electron interaction dominates over electron–phonon interactions, we proceed now and investigate the role of equilibrium distributions other than Fermi–Dirac distributions in laser performance. As

we have shown in previous sections, there are finite flux equilibria, for which there is a finite and constant flux of carriers and energy across a given spectral window. It is the aim of this work to suggest that these finite flux equilibria are more relevant to situations in which energy and carriers are added in one region of the spectrum, redistributed via collision processes to another region where they are absorbed. In conventional diode lasers, pumping is a process in which charge carriers are injected into the depletion layer region in a p-n or p-i-n structure (see, e.g., [25]). If the active layer is bulk-like, this process is based on a regular drift–diffusion current, whereas in quantum-well lasers there is the additional process of carrier capture into the quantum well by means of inelastic scattering processes. In the following we restrict ourselves to the simplest model for injection pumping that neglects the intrinsically anisotropic aspect of injection pumping but includes the basic features of Pauli blocking effects in the pump process [24]. Within this model, the rate of change of the carrier distribution is proportional to $\Lambda_k(1-n_k)$, where the pump coefficient Λ_k is taken as a Fermi function with a given density modeling the incoming equilibrated carriers, n_k is the actual carrier distribution in the active region, and $(1-n_k)$ takes into account the Pauli blocking effects. This means that only non-occupied states can be filled by the pump current. Since Λ_k is a function that extends over a large range of k-values, we call this pump model "broad-band pumping". In contrast to broad-band pumping one can also pump a laser locally in momentum space. However, usually such a local pump process is narrow-band optical pumping, but this is not commonly used to pump semiconductor lasers. There are, however, also electrical pumping schemes available, which are based on tunneling processes, and which, in principle, can allow for selective and localized pumping and damping (see, e.g., [26]).

In the following we will examine the laser process and discuss, in particular, the influence of the pumping process and its relation to the equilibrium distribution function in stationary laser operation. We base our numerical solutions on a greatly simplified laser model. We assume that the distribution functions for electrons and holes are identical (in other words, we assume electrons and holes to have identical effective masses); we model the cavity losses by a simple phenomenological loss term in the propagation equation for the light field amplitude; we assume ideal single-mode operation; we make the rotating wave approximation in the equation for the distribution functions and the optical polarization function p_k; we neglect all electron–hole Coulomb correlations (the so-called Coulomb enhancement, see, e.g., [24]); we neglect bandgap energy renormalization; and we neglect, as mentioned above, electron–phonon interaction. In spite of the approximations made, our model still captures the basic processes in a semiconductor laser. The equations of motion (a form of the semiconductor Maxwell–Bloch equations, see, e.g., [24,27]) read:

$$\frac{\partial e}{\partial t} = \mathrm{i}\frac{\Omega}{2\epsilon_0}\frac{V}{(2\pi)^d}\int \mu_k p_k \,\mathrm{d}\mathbf{k} - \gamma_E e, \tag{5.1}$$

$$\frac{\partial p_k}{\partial t} = (\mathrm{i}\Omega - \mathrm{i}\tilde{\omega}_k - \gamma_P)p_k - \frac{\mathrm{i}\mu_k}{2\hbar}(2n_k - 1)e, \tag{5.2}$$

$$\frac{\partial n_k}{\partial t} = \Lambda_k(1-n_k) - \gamma_k n_k + \left(\frac{\partial n_k}{\partial t}\right)_{\text{collision}} - \frac{\mathrm{i}}{2\hbar}\left(\mu_k p_k e^* - \mu_k p_k^* e\right). \tag{5.3}$$

Here $e(t)$ and $p_k(t)$ are the electric field and polarization (at momentum $\mathbf{k}$) envelopes of the carrier wave $\exp(-\mathrm{i}\Omega t + \mathrm{i}Kz)$, where Ω is the cavity frequency (we assume single mode operation only) and n_k is the distribution function for electrons and holes. The constants $\gamma_E = 6\times 10^{10}/\mathrm{s}^{-1}$, $\gamma_P = 10^{13}/\mathrm{s}^{-1}$ model electric field losses and polarization decay (dephasing), ϵ_0 is the dielectric constant, μ_k is the weighting accorded to different $\mathbf{k}$ momentum values and is modeled by $\mu_k = \mu_{k=0}/(1+\epsilon_k/\epsilon_{\text{gap}})$, $\mu_{k=0} = 3/10^{10}\,Me$, e is the electron charge, $\gamma_k = 10^{10}\,\mathrm{s}^{-1}$ represent non-radiative carrier damping. In (5.3), Λ_k is the pumping due to the injection current (taken to be between 0.001 and 0.01 ps^{-1}) and in (5.2) $\hbar\tilde{\omega}_k = \epsilon_{\text{gap}} + \epsilon_{e,k} + \epsilon_{h,k}$. We further assume that all fields are isotropic and make a convenient transformation from k $(= |\mathbf{k}|)$ to ω via the dispersion relation $\omega = \omega(\mathbf{k})$ defining the carrier density $n_\omega = n(k(\omega))$ and approximate the collision term $(\partial n_k/\partial t)_{\text{collision}} = (\partial n_{k(\omega)}/\partial t)_{\text{collision}}$ by the differential kinetic

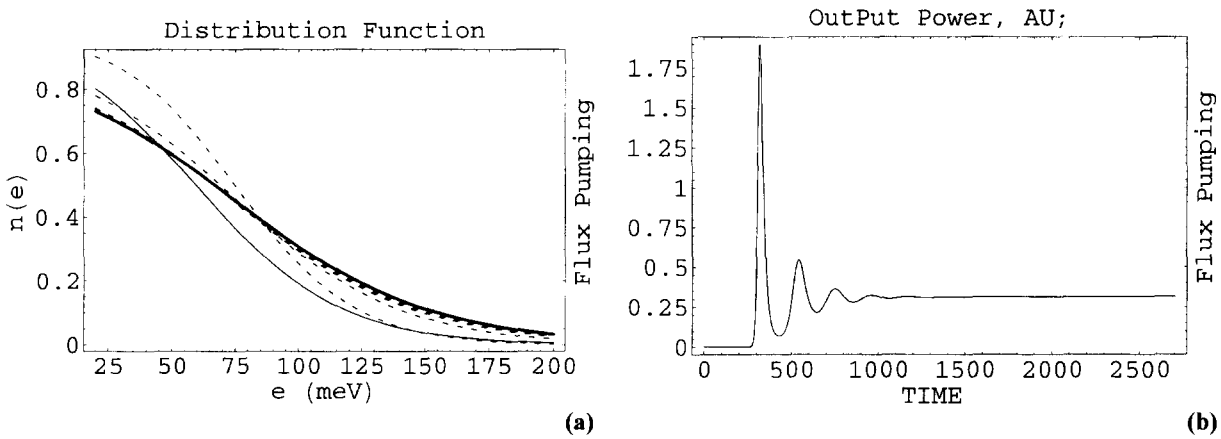

Fig. 4. Time dependence of distributions (a) and laser intensity (b) according to (5.1)–(5.4). Local-band pumping is modeled by specifying the carrier and energy flux rates Q_L and $P_L = -\omega_L Q_L$ at the right ($\omega_0 \simeq 200$ meV) boundary. The initial distribution function (shown by a thin line in this and consequent figures) evolves through a number of intermediate states shown by dashed lines, until the laser switches on. The final (steady) distribution function is shown by a thick solid line (in this and subsequent figures). Time is given in units of the relaxation time $\tau_{relax} = 100$ fs on this and subsequent figures. The laser fails to switch on in the broad-band pumping case for these levels of pumping.

expression (4.7):

$$\left(\frac{\partial n_{k(\omega)}}{\partial t}\right)_{\text{collision}} = -\frac{1}{\Omega_0 k^{d-1}(\mathrm{d}k/\mathrm{d}\omega)}\frac{\partial^2}{\partial\omega^2}\left[\left(n_\omega^4\frac{\partial^2}{\partial\omega^2}\left(\frac{1}{n_\omega}\right)+n_\omega^2\frac{\partial^2}{\partial\omega^2}(\ln(n_\omega))\right)\times I\times\omega^s\right]. \tag{5.4}$$

We choose the value of the constant I to ensure that a solution of (5.4) relaxes with relaxation time of 100 fs to its equilibrium value and s is taken to be 7.

We now compare the laser efficiencies in two numerical experiments in which we arrange to: (i) Pump broadly across a wide range of momenta, so that the effective carrier distribution equilibrium has zero (or small [5]) flux. We take the pump profile to be given by the Fermi–Dirac distribution. (ii) Pump carriers and energy into a narrow-band of frequencies about ω_0 and simulate this by specifying carrier and energy flux rates Q_L and $P_L = -\omega_L Q_L$ at the boundary $\omega = \omega_0$. P_L is chosen so that the energy absorbed by the laser is consistent with the number of carriers absorbed there. $\omega = \omega_L < \omega_0$ is the frequency at which the system lases. We compare only cases in which the total amount of energy supplied is approximately the same. Owing to the distribution of the supply, the particle number in the broad-band pumping has to be higher.

In the first numerical experiment, we show that for a very small amount of pumping the laser operates for the narrow-band pumping, while it fails to operate in the broad-band pumping case (i.e., the threshold pumping value for narrow-band pumping is much lower than in the broad-band case). The carriers supplied through the pumping process get totally absorbed by the global damping $-\gamma_k n_k$ in the broad-band pumping case. There no lasing occurs. In the local-band pumping case, for the same amount of energy and lower amount of particle supplies, the laser operates. This is the qualitative difference between two cases.

[5] Even for broad-band pumping the small amount (much smaller than in local band pumping) of P and Q fluxes is also excited, because the form of the pumping f_k gets effectively multiplied by the Pauli blocking $(1-n_k)$ term. But these fluxes are much smaller and relatively local in k space.

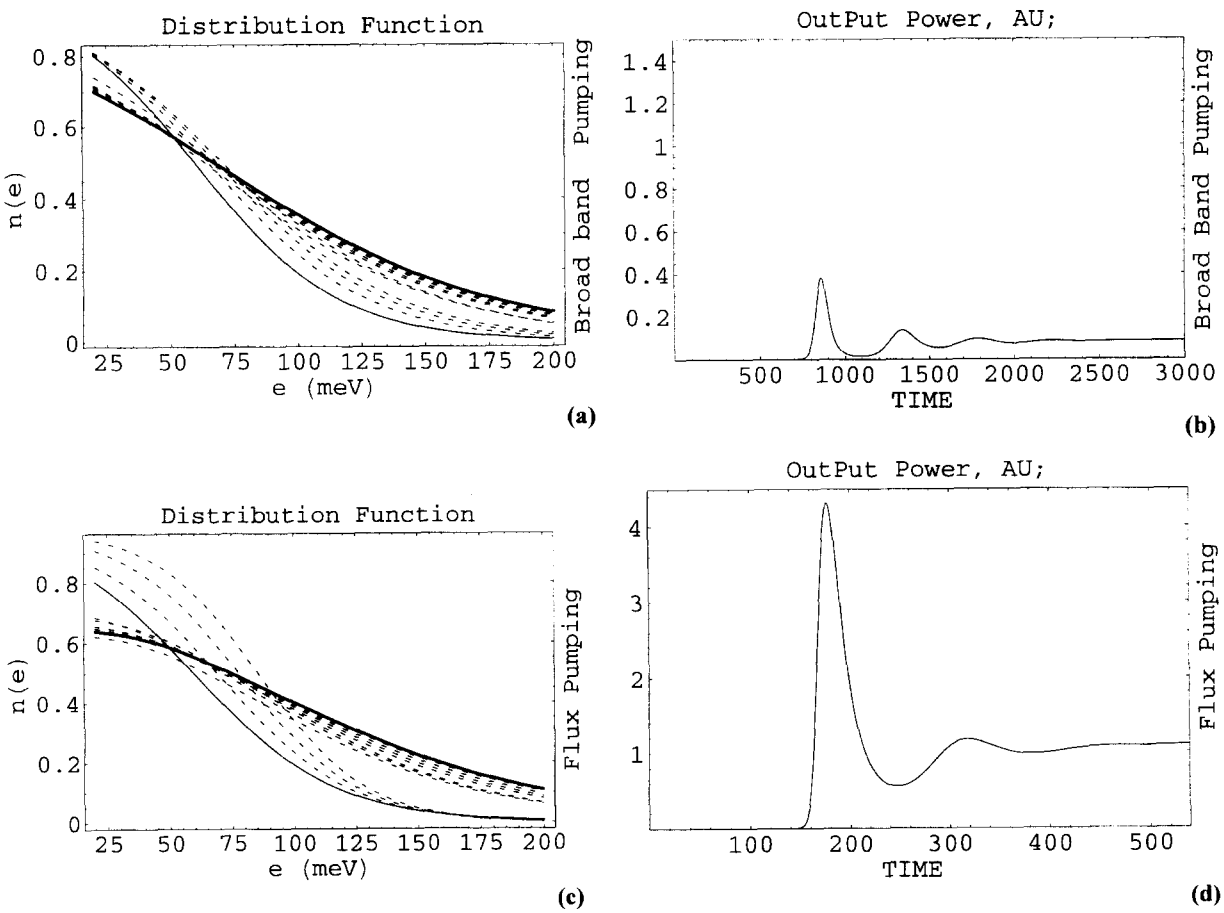

Fig. 5. Same as in Fig. 4 but for increased pump rate: (a) broad-band pumping; (b) narrow-band pumping with $\omega_0 \simeq 200$ meV.

The results of this numerical experiment are presented in Fig. 4. The narrow-band pumped laser switches on and generates a non-zero output power. We pump in the narrow region around $\omega_0 \simeq 200$ meV and we model this by specifying the boundary conditions at ω_0 to correspond to carrier and energy flux rates Q_L and $P_L = -\omega_L Q_L$, respectively. The initial value of the distribution function (shown by a thin line), taken to be just below the lasing threshold, builds up because of the influx of particles and energy from the right boundary (dashed lines) until the laser switches on. The final (steady) distribution function is shown by a thick solid line and corresponds to a flux of particles and energy from the right boundary (where we add particles and energy) to the left boundary, where the system lases (Fig. 4(a)). The output power as a function of time is also shown (Fig. 4(b)). Time is measured in units of relaxation times $\tau_{relax} = 100$ fs. In the contrast, the broad-band pumped laser fails to switch on for such weak pumping.

We then increase the level of pumping, to a point where the laser turns on for both the broad-band and narrow-band pumping cases, and examine the output power in both cases. It turns out that for the same amount of energy pumped, [6]

[6] More carriers are pumped in the case of broad-band pumping because of the pump distribution. Because there are fewer carriers in the narrow-band pumping case, the "effective" chemical potential also decreases, which increases efficiency.

and for almost the same amount of carriers pumped the output power in the narrow-band case is significantly higher than in the broad-band case. The results are presented in Fig. 5. We first pump broadly, so that the effective carrier distribution has (almost) zero flux. The initial distribution function (thin line, Fig. 5(a)) builds up because of a global pumping (dashed lines) until the laser switches on. The final (steady) distribution function is shown by the thick solid line. The output power as a function of time is also shown (Fig. 5(b)).

If we pump in the narrow region around $\omega_0 \simeq 200\,\mathrm{meV}$ and we model this by specifying the carrier and energy flux rates Q_L and $P_L = -\omega_L Q_L$, then the initial distribution function (thin line) builds up because of an influx of particles and energy from the right boundary (dashed lines) until the laser switches on. The final (steady) distribution function is shown by a thick solid line and corresponds to a flux of particles and energy from the right boundary (where we add particles and energy) to the left boundary, where the system lases (Fig. 5(c)). The output power as a function of time is also shown (Fig. 5(d)).

These results certainly suggest that the possibility of using narrow-band pumping and the resulting finite flux equilibrium of the QKE is an option which is worth exploring further.

6. Conclusions

We have shown that, for weak coupling, the full BBGKY hierarchy of operator equations has a natural asymptotic closure consistent with Hartree–Fock factorization and complex frequency renormalization.

We have demonstrated that the QKE has a new class of steady (equilibrium) solutions which carry constant fluxes of particles and energy across momentum space. We have explored these solutions by using the differential approximation to the collision integral.

We have then applied these ideas to semiconductor lasers and shown that the output power is much higher when the finite flux equilibrium is excited. While we do not claim that, if we take all effects into account, the advantages of narrow-band pumping will necessarily remain, we do suggest that the evidence suggests that it is a possibility worth pursuing further.

Acknowledgements

The authors wish to thank the Arizona Center for Mathematical Sciences (ACMS) for support. ACMS is sponsored by AFOSR contract F49620-97-1-0002 under the University Research Initiative Program at the University of Arizona, Department of Mathematics.

Appendix A. Diagrams

In this section we present simple diagrams which can help one to visualize the definition of cumulants. These diagrams are only meant as an aid to visualize the correlation contribution and should not be confused with other diagrams such as Feymann diagrams. The following pictures are intended to illustrate the ways to factorize N_{1234}, N_{123456} and $N_{12345678}$. Let us denote by square boxes operator averages according to (2.9), so that two connected arrows present ρ (2 operator expectation value), and

$N_{1234} =$ 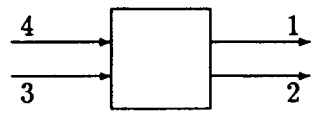

Let us present cumulants in the form of vertices, with incoming arrows representing the arguments of annihilation operators, and the outgoing the arguments of creation operators. Then the second order cumulant (which is the same as the two operator average) is represented by two arrows:

$\rho_1\delta_2^1 =$ 

The fourth order cumulant is represented by four arrows:

$\mathcal{P}_{1234} =$ 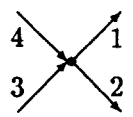

so that the definition of fourth order cumulant $\mathcal{P}_{1234}$ is

$$N_{1234} = \rho_1\rho_2(\delta_3^2\delta_4^1 - \delta_4^2\delta_3^1) + \mathcal{P}_{1234}\delta_{34}^{12}. \tag{A.1}$$

This partition can be represented graphically as

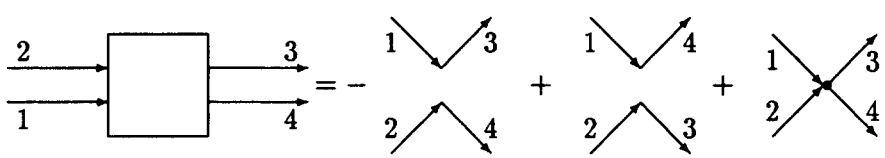

Owing to the commutation relations (2.1), if we interchange two indices corresponding to two creation or two annihilation operators, the average should change its sign, e.g., $N_{1234} = -N_{2134}$. The definitions of cumulants should not contradict this property, so each product of lower order cumulants should be either positive or negative, depending upon whether it corresponds to an odd or even permutation. This explains the negative sign in the form of $\rho_1\rho_2\delta_4^2\delta_3^1$ term in (A.1). Similarly, the definition of the sixth order cumulant $\mathcal{Q}_{123456}$ is

$$\begin{aligned} N_{123456} = {} & \rho_1\rho_2\rho_3 \cdot (\ \delta_4^3(\delta_5^2\delta_6^1 - \delta_5^1\delta_6^2) + \delta_5^3(\delta_6^2\delta_4^1 - \delta_4^2\delta_6^1) + \delta_6^3(\delta_5^1\delta_4^2 - \delta_4^1\delta_5^2)\ ) \\ & + \rho_3[+\mathcal{P}_{1256}\delta_4^3\delta_{56}^{12} - \mathcal{P}_{1246}\delta_5^3\delta_{46}^{12} + \mathcal{P}_{1245}\delta_6^3\delta_{45}^{12}] \\ & + \rho_2[-\mathcal{P}_{1356}\delta_4^2\delta_{56}^{13} + \mathcal{P}_{1346}\delta_5^2\delta_{46}^{13} - \mathcal{P}_{1345}\delta_6^2\delta_{45}^{13}] \\ & + \rho_1[+\mathcal{P}_{2356}\delta_4^1\delta_{56}^{23} - \mathcal{P}_{2346}\delta_5^1\delta_{46}^{23} + \mathcal{P}_{2345}\delta_6^1\delta_{45}^{23}] + \mathcal{Q}_{123456}\delta_{456}^{123}. \end{aligned} \tag{A.2}$$

This partition can be represented as

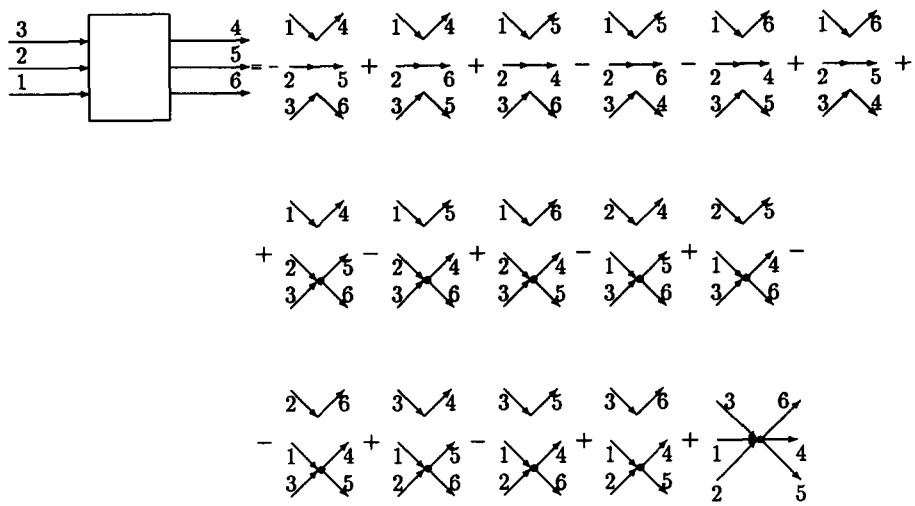

Again, because of the commutation relations (2.1), if we interchange two indices corresponding to two creation or two annihilation operators, the average should change its sign, e.g., $N_{123456} = -N_{213456}$. The picture below illustrates a simple algorithm of counting the parity of permutation by counting the number of crossing between lines connecting different arguments. In the example below, one sees that the parity of $n_1\delta_5^1\mathcal{P}_{2346}$ term in the expansion of N_{123456} is odd (because of the odd number of crossings), so the product is negative.

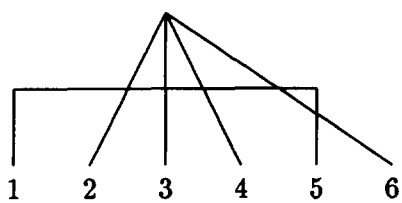

In the same manner, the definition of $\mathcal{Q}_{12345678}$

$$N_{12345678} = \rho_1\rho_2\rho_3\rho_4(\delta_5^4\delta_6^3\delta_7^2\delta_8^1 + \cdots)\rho_4\mathcal{Q}_{123678}\delta_5^4 + \cdots + \rho_1\rho_2\mathcal{P}_{3456}\delta_8^1\delta_7^2 + \cdots + \mathcal{P}_{3456}\mathcal{P}_{1278} + \cdots + \mathcal{R}_{12345678} \tag{A.3}$$

can be presented as

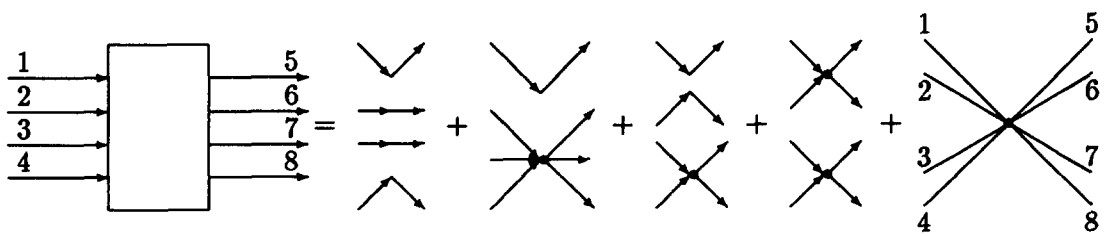

Owing to the large amount of terms in this case, we show only schematically the factorization of $N_{1'2'3'4'5'6'7'8'}$. One has to choose *all* possible permutations of indices, corresponding to different topologies putting "annihilation" arguments to the incoming and "creation" arguments to the outgoing arrows.

References

[1] L.D. Landau, E.M. Lifshitz, Physical Kinetics, Pergamon Press, New York, 1981.
[2] L.P. Kadanoff, G. Baym, Quantum Statistical Mechanics, Addison-Wesley, New York, 1989.
[3] P.P.J.M. Schram, Kinetic Theory of Gases and Plasmas, Kluwer Academic Publishers, Dordrecht, 1991.
[4] D.F. Dubois, in: W.E. Brittin (Ed.), Lectures in Theoretical Physics, vol. IX c, Gordon and Breach, New York, 1967, pp. 469–620.
[5] Y.L. Klimontovich, D. Kremp, W.D. Kraeft, Adv. Chem. Phys. 68 (1987) 175.
[6] P. Danielewicz, Ann. Phys. 152 (1984) 239.
[7] A. Balescu, Phys. Fluids 3 (1960) 52.
[8] A. Lenard, Ann. Phys. (N.Y.) 3 (1960) 390.
[9] W.D. Kraeft, D. Kremp, W. Ebeling, G. Röpke, Quantum Statistics of Charged Particle Systems, Akademie Verlag, Berlin, 1986.
[10] L.P. Kadanoff, G. Baym, Quantum statistical mechanics, Green's function methods in equilibrium problems.
[11] H.S. Köhler, Phys. Rev. E 53 (1996) 3145.
[12] P. Lipavski, V. Spica, Phys. Rev. B 52 (1995) 14615; Phys. Rev. Lett. 73 (1994) 3439.
[13] K.E. Sayed, L. Banyai, H. Haug, Phys. Rev. B 50 (1994) 1541.
[14] A.V. Kuznetsov, Phys. Rev. B 44 (1991) 8721.
[15] V.E. Zakharov, V.S. L'vov, G.Falkovich, Kolmogorov Spectra of Turbulence, Springer, Berlin, 1992.
[16] S. Dyachenko, A.C. Newell, A. Pushkarev, V.E. Zakharov, Physica D 57 (1992) 96–160.
[17] S. Hasselmann, K. Hasselmann, J.H. Allender, T.P. Barnett, J. Phys. Oceonogr. 15 (1985) 1378.
[18] A.M. Balk, J. Fluid Mech. 315 (1996) 139.
[19] B.J. Benney, A.C. Newell, Stud. in Appl. Math. 48 (1) (1969) 29.
[20] A.C. Newell, Rev. Geophy. 6 (1968a) 1.
[21] D.J. Benney, P. Saffman, Proc. Roy. Soc. A 289 (1966) 301–320.
[22] V.E. Zakharov, Zh. Priklad. Tech. Fiz. 1 (1965) 35; J. Appl. Mech. Tech. Phys. 1 (1967) 22.
[23] V.E. Zakharov, Zh. Eksp. Teor. Fiz. 51 (1966) 688; Sov. Phys. JETP 24 (1967).
[24] W.W. Chow, S.W. Koch, M. Sargent, Semiconductor Laser Physics, Springer, Berlin, 1994.
[25] P. Bhattacharya, Semiconductor Optoelectronic Devices, Prentice-Hall, Englewood Cliff, NJ, 1994.
[26] X. Zhang, Y. Yuan, P. Bhattacharya, Appl. Phys. Lett. 69 (1996) 2309.
[27] H. Haug, S.W. Koch, Quantum Theory of the Optical and Electronic Properties of the Semiconductors, 2nd ed., World Scientific, Singapore, 1993.
[28] A.M. Balk, A. Pushkarov, unpublished (1991).